NAVAL POSTGRADUATE SCHOOL

MONTEREY, CALIFORNIA

THESIS

THE FORMATION AND INTENSIFICATION OF HURRICANE DELTA 2020

by

Chelsey B. Huff

September 2023

Thesis Advisor: Michael T. Montgomery
Second Reader: Mark A. Boothe

THIS PAGE INTENTIONALLY LEFT BLANK

REPORT DOCUMENTATION PAGE	*Form Approved OMB No. 0704-0188*

1. AGENCY USE ONLY *(Leave blank)*	**2. REPORT DATE** September 2023	**3. REPORT TYPE AND DATES COVERED** Master's thesis

4. TITLE AND SUBTITLE THE FORMATION AND INTENSIFICATION OF HURRICANE DELTA 2020	**5. FUNDING NUMBERS**
6. AUTHOR(S) Chelsey B. Huff	
7. PERFORMING ORGANIZATION NAME(S) AND ADDRESS(ES) Naval Postgraduate School Monterey, CA 93943-5000	**8. PERFORMING ORGANIZATION REPORT NUMBER**
9. SPONSORING / MONITORING AGENCY NAME(S) AND ADDRESS(ES) N/A	**10. SPONSORING / MONITORING AGENCY REPORT NUMBER**

11. SUPPLEMENTARY NOTES The views expressed in this thesis are those of the author and do not reflect the official policy or position of the Department of Defense or the U.S. Government.

12a. DISTRIBUTION / AVAILABILITY STATEMENT Approved for public release. Distribution is unlimited.	**12b. DISTRIBUTION CODE** A

13. ABSTRACT (maximum 200 words)

This thesis investigates the formation and rapid intensification periods of Hurricane Delta from the late 2020 Atlantic hurricane season using the marsupial pouch paradigm. The paradigm proposes the existence of a quasi-closed region with a recirculating flow called a "pouch" that protects the precursor of a tropical cyclone as it travels across the Atlantic Ocean and into the Caribbean Sea. Global model analyses in the co-moving and earth-relative framework are used to track Delta's precursor. A deeper investigation into the precursor's stalling and alignment, rapid intensifications, and a rapid weakening event of Delta is examined by using multiple variables, including moisture, relative vorticity, Okubo-Weiss, and vertical wind shear.

14. SUBJECT TERMS Hurricane Delta, marsupial paradigm, wave pouch, rapid intensification	**15. NUMBER OF PAGES** 81
	16. PRICE CODE

17. SECURITY CLASSIFICATION OF REPORT Unclassified	**18. SECURITY CLASSIFICATION OF THIS PAGE** Unclassified	**19. SECURITY CLASSIFICATION OF ABSTRACT** Unclassified	**20. LIMITATION OF ABSTRACT** UU

NSN 7540-01-280-5500

Standard Form 298 (Rev. 2-89)
Prescribed by ANSI Std. 239-18

THIS PAGE INTENTIONALLY LEFT BLANK

Approved for public release. Distribution is unlimited.

THE FORMATION AND INTENSIFICATION OF HURRICANE DELTA 2020

Chelsey B. Huff
Second Lieutenant, United States Air Force
BA, University of North Texas, 2021

Submitted in partial fulfillment of the
requirements for the degree of

MASTER OF SCIENCE IN METEOROLOGY

from the

NAVAL POSTGRADUATE SCHOOL
September 2023

Approved by: Michael T. Montgomery
Advisor

Mark A. Boothe
Second Reader

Wendell A. Nuss
Chair, Department of Meteorology

THIS PAGE INTENTIONALLY LEFT BLANK

ABSTRACT

This thesis investigates the formation and rapid intensification periods of Hurricane Delta from the late 2020 Atlantic hurricane season using the marsupial pouch paradigm. The paradigm proposes the existence of a quasi-closed region with a recirculating flow called a "pouch" that protects the precursor of a tropical cyclone as it travels across the Atlantic Ocean and into the Caribbean Sea. Global model analyses in the co-moving and earth-relative framework are used to track Delta's precursor. A deeper investigation into the precursor's stalling and alignment, rapid intensifications, and a rapid weakening event of Delta is examined by using multiple variables, including moisture, relative vorticity, Okubo-Weiss, and vertical wind shear.

THIS PAGE INTENTIONALLY LEFT BLANK

TABLE OF CONTENTS

THIS PAGE INTENTIONALLY LEFT BLANK

LIST OF FIGURES

LIST OF TABLES

THIS PAGE INTENTIONALLY LEFT BLANK

LIST OF ACRONYMS AND ABBREVIATIONS

ACE	accumulated cyclone energy
AEW	African easterly wave
AMO	Atlantic multidecadal oscillation
ELI	ENSO longitude index
ENSO	El Niño Southern Oscillation
GFS	Global Forecasting System
IR	infrared
MJO	Madden-Julian oscillation
MP	Marsupial Paradigm
NCEP	National Center for Environmental Prediction
NHC	National Hurricane Center
NOAA	National Oceanic and Atmospheric Administration
OW	Okubo-Weiss
PI	potential intensity
RH	relative humidity
RI	rapid intensification
SST	sea surface temperature
TC	tropical cyclone
TD	tropical depression
UTC	universal time coordinated

THIS PAGE INTENTIONALLY LEFT BLANK

ACKNOWLEDGMENTS

This endeavor would have not been possible without the encouragement and support of my advisory team, Dr. Michael T. Montgomery and Mr. Mark Boothe. I am grateful for the guidance, tireless help, and advice from the start of our journey all the way to the end.

I am also grateful to my cohort partner and roommate, 2d Lt Nicohl Corretjer, for her support. We have pushed ourselves and each other to be the best and I hope we will continue to do so for the rest of our careers. Lastly, I would be remiss in not mentioning the love and support from my family members and my fiancé, Bryce.

THIS PAGE INTENTIONALLY LEFT BLANK

I. INTRODUCTION

A. MOTIVATION

In the United States over the past 41 years, tropical cyclones (TC) have cost over $1.1 trillion (averaging $20.5 billion per event) in damages and are responsible for 6,697 deaths (NOAA), making TCs the most damaging and deadliest weather disaster in the United States. All uniformed services are threatened each hurricane season by the potential billions of dollars in damages to bases, aircraft, ships, and equipment. As a notable example, Hurricane Michael (2018) wreaked havoc on Tyndall Air Force Base, damaging 95% of the buildings on base, including on-base housing and some of the 17 F-22 raptors that could not be flown out due to timing or inability to fly. A majority of Tyndall AFB needed to be rebuilt, taking several years and at least $5 billion. Hurricane Florence (2017) caused a total of $3.6 billion worth of damages at the Marine Corps Base Camp Lejeune, not including the cost of damages to military housing. All hurricanes cause the displacement, injury, or death of people and damage or destruction of buildings, homes, businesses, services, and equipment, which reduces the operational readiness of all uniformed services and the ability to provide humanitarian aid to civilians and military services alike.

Currently, after a hurricane forms, operational forecasters can skillfully predict its path 3–5 days in advance (Samost 2006). However, before forecasters can produce accurate hurricane forecasts, they must accurately anticipate hurricane formation. A confounding subset of hurricanes are those that form in the Caribbean. Their formation in such proximity to continental United States military installations results in reduced forecast lead time that does not allow for adequate base protection measures, sorties, and evacuations.

Late in the 2020 Atlantic hurricane season, an African easterly wave (AEW) traversed the entire Atlantic before formation as a tropical depression (TD) in the Caribbean. This storm developed into Hurricane Delta, experiencing a period of rapid intensification during the process. By examining the formation of the tropical cyclone that became Hurricane Delta with the concepts of the Marsupial Paradigm (MP), we hope to

gain a greater understanding of the dynamics and thermodynamics that are relevant to the formation and intensification of hurricanes.

B. THE MARSUPIAL PARADIGM

The MP is a conceptual framework introduced by Dunkerton, Montgomery, and Wang (2009; hereafter DMW09) to describe how a hybrid diabatic Rossby wave/vortex (within the wave critical layer or in isolation) may develop into a TD and possibly later develop into a tropical storm or even hurricane. A key component of the MP is the transformation from the Earth-relative to a Lagrangian (co-moving) reference frame. The transformation into the co-moving reference frame allows for a feature-relevant diagnosis of TC formation that is superior to the Earth-relative framework.

Figure 1 depicts a schematic summary of the components of the MP and how these components interact. The critical latitude or level (labeled "Latitude line") is where the mean flow and wave phase speed in the direction of wave propagation are equal. The pouch begins to form along the trough of a tropical wave (labeled "Axis of tropical wave") and the critical latitude, and the pouch region is the interior of the solid black line with arrows, which is warm and moist, propagating westward with the tropical wave and protecting the interior from lateral dry air or dust intrusion from the Sahara Air Layer. This protection allows for the development of a storm inside of the pouch, which can gradually strengthen and intensify to become a TC. Pouches are frequently visible in the co-moving framework and allow for an analysis of the flow kinematics, dynamics and thermodynamics in and around the pouch.

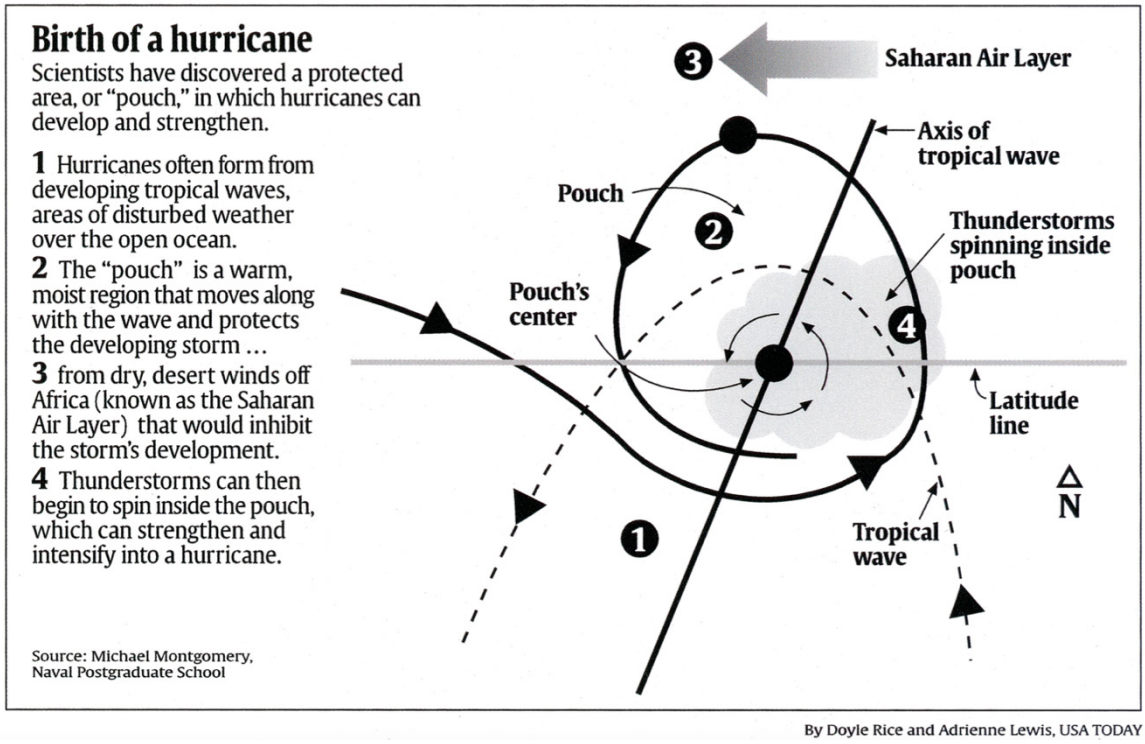

A graphical depiction and description of marsupial pouch development creating a conducive environment for tropical cyclone formation. This graphic shows the trough axis (axis of a tropical wave), critical latitude (latitude line), and tropical wave.

Figure 1. Marsupial paradigm graphic. Source: Rice (2008).

The MP provides a key ingredient in the genesis of hurricanes as the "pouch" allows for a protective region within the developing tropical wave over the open ocean, where the local wind speed surrounding the new pouch center is similar to the translation speed of the tropical wave. In DMW09, they were able to document that 55 out of 61 tropical disturbances, which developed into tropical storms during August and September from 1998 to 2001, had a protective pouch. These 55 storms revealed that while critical layers sometimes resemble the ideal east-west train of cat's eyes, they are often less regular and have one or more recirculation regions in the co-moving frame.

Each of the storms studied by DMW09 came from easterly waves that were propagating westward across the Atlantic and eastern Pacific basins. All 55 wave/genesis events were examined and led to the following two main conclusions: (i) In the co-moving frame, there was persistent convective precipitation that occurred in a quasi-closed

recirculating gyre; and (ii) the development of the tropical depression occurred near the intersection of the critical latitude and the trough axis (Dunkerton et al. 2009). The study of DMW09 was predicated on three main hypotheses (H1-H3).

> (H1) Proto-vortex cyclonic eddies instrumental in TC formation are intimately associated with the parent wave's critical latitude in the lower troposphere. The critical layer and Kelvin cat's eye within, formed as a result of the wave's finite-amplitude interaction with its own critical latitude, contain a region of cyclonic rotation and weak straining/shearing deformation in which synoptic waves and mesoscale vorticity anomalies, moving westward together, amplify and aggregate on a nearly zero relative mean flow. This multi-scale interaction provides a dynamical pathway to "bottom-up" development of the proto-vortex from below. (Dunkerton et al. 2009, p. 5594)

The first hypothesis implies that TC genesis occurs within the critical layer of the parent wave in the lower troposphere. The bottom-up development in this hypothesis occurs in the region surrounding a nonlinear wave's critical level when the convective heating profile has one or more hot vortical towers. The deep vortical convection is initiated by Ekman-like convergence that is induced by boundary-layer drag and/or low-level convergence from a convective heating profile (DMW09).

> (H2) The critical-layer cat's eye of the parent wave provides a set of quasi-closed material contours inside of which air is repeatedly moistened by convection, protected to some degree from lateral intrusion of dry air and impinging vertical shear, and (thanks to its location near the critical latitude) able to keep pace with the parent wave until the proto-vortex has strengthened into a self-maintaining entity. ((Dunkerton et al. 2009, p. 5594)

The primary focus of the second hypothesis is the protection that a proto-vortex gets from dry or dusty air from the outside air and the supply of repeatedly moistened air via convection within the pouch. Inside the quasi-closed streamlines, convective activity enables parcels to become irreversibly entrained into the gyre and concentrate vorticity in such a way that provides enhanced protection from lateral dry air intrusion from outside of the pouch. The convection then becomes focused at a "sweet spot" where the critical latitude and trough axis intersect.

> (H3) The parent wave is maintained and possibly enhanced by diabetically amplified eddies within the wave (proto-vortices on the mesoscale), a process favored in regions of small intrinsic phase speed. ((Dunkerton et al. 2009, p. 5597)

The third hypothesis is that the parent wave is maintained and possibly enhanced by the eddies within the wave by diabatic heating. The amplification of the pouch by diabatic heat sources within it is to be expected in regions of small intrinsic phase speed. The OW parameter is a key variable used by the Montgomery Research Group to track pre-TC disturbances. The OW parameter is "a measure of the shape preserving component of vortical flow" (DMW09 p.5639). Since the sign of the OW parameter can be arbitrarily selected, positive OW is selected herein to indicate the vorticity dominant and shape preserving region. Negative OW is then indicative of vorticity filamentation that is associated with shearing deformation and straining deformation. Mathematically, for non-divergent flow the OW parameter is given by the equation:

$$OW = \zeta^2 - S_1^2 - S_2^2 = \left(V_x - U_y\right)^2 - \left(U_x - V_y\right)^2 - \left(V_x + U_y\right)^2 \quad (1)$$

In equation (1), $\zeta = V_x - U_y$ represents the relative vertical vorticity (the rotational flow), while S_1 and S_2 represent the horizontal strain deformation and horizontal shear deformation, respectively. By squaring each value, the magnitude of the signal is amplified, thereby aiding the analysis. The OW for real-case, pre-TC, disturbance events have typical values on the order of $10^{-9}s^{-2}$.

To recap: In this thesis, positive values of OW are indicative of rotationally dominant flow and negative values are indicative of strain or shear dominant flow. Areas of positive OW are associated with the potential for tropical cyclogenesis. Because deep convection collectively acts to draw cyclonic vorticity inward in the lower troposphere, a persistent influx of cyclonic vorticity will generally lead to increased vorticity in the central region of the pouch and a relatively high OW parameter near the sweet spot of the pouch.

The pioneering work of DMW09 was repeated independently by Asaadi et al. (2015a,b and 2017), and the foregoing conclusions were affirmed by these investigators. Asaadi et al. also found that: (i) all tropical storms and hurricanes were associated with

tropical easterly waves from the Atlantic and eastern Pacific from August-September 1998–2001; (ii) nonlinear dynamical and thermodynamical processes play a synergistic role for the formation processes of a cat's eye and easterly waves that produce named storms; and (iii) waves on a critical latitude do not develop into named storms when the Okubo-Weiss (OW) has a large negative value. While these authors verified the findings of DMW09, their focus was on the early formation of the critical layer. Notably, they presented and verified a novel explanation for the approximate 25% rate of TD formation from tropical disturbances in the main development region.

C. LATE 2020 ATLANTIC HURRICANE SEASON CONDITIONS

October and November were unusually active in the 2020 Atlantic hurricane season. During the 2020 season there were 20 named storms, 14 hurricanes, and seven major hurricanes (Category 3+ on the Saffir-Simpson Hurricane Wind Scale). Overall, there were highly favorable conditions for TC development, such as the Madden-Julian oscillation (MJO) index, La Niña, low vertical wind shear, above average sea surface temperature (SST), and moisture all contributing to this active hurricane season.

Tropical cyclone development in the main development region (MDR), which is defined as the area between 5°-25°N and 15°-60°W, occurs most often during the real-time multivariable MJO (RMM) phases 1, 2, and 5 (Ventrice et al. 2011). With the MJO index staying in phase 5 for most of October (Figure 2a), most likely due to a stationary region of enhanced convection near the South China Sea, the likelihood of late season hurricane activity was increased (Klotzbach et al. 2022). Figure 2a is divided into 8 different phases, where enhanced convection (and associated rainfall) develops and propagates eastward. Phase 1 represents the development of enhanced convection over the western Indian Ocean. Phases 2 and 3 represent the eastward movement of the enhanced convection over Africa, the Indian Ocean, and parts of the subcontinent of India. Phases 4 and 5 represent the enhanced convection when it has reached Indonesia and the West Pacific. Phases 6, 7, and 8 represents the enhanced convection as it moves over the western Pacific and eventually dies out.

The stationary region of the 200 hPa velocity potential anomaly, indicated by the purple ellipse in Figure 2b, is thought to be a favorable contributor to the formation of hurricanes in the Caribbean as the MJO index remained in phase 5 for approximately 30 days. This stationary pattern was associated with an intensifying La Niña circulation and appears to be the primary sub-seasonal driver during October. The foregoing interpretation is supported by Klotzbach et al. who wrote (p. E110): The "anomalously low wind shear in the western Caribbean and Gulf of Mexico, likely driven by a moderate-intensity La Niña event and anomalously high sea surface temperatures in the Caribbean, provided dynamic and thermodynamic conditions that were much more conducive than normal for late-season tropical cyclone formation and rapid intensification."

La Niña is generally thought to contribute to an increase in the Atlantic hurricane activity by weakening the vertical wind shear located over the Caribbean Sea and tropical Atlantic Basin, and allowing storms to develop and intensify (NOAA 2020). The 2020 strength of the La Niña event reached its peak in October 2020, and its peak value was determined by the in-phase amplification of all time scale variations (Li et al. 2022).

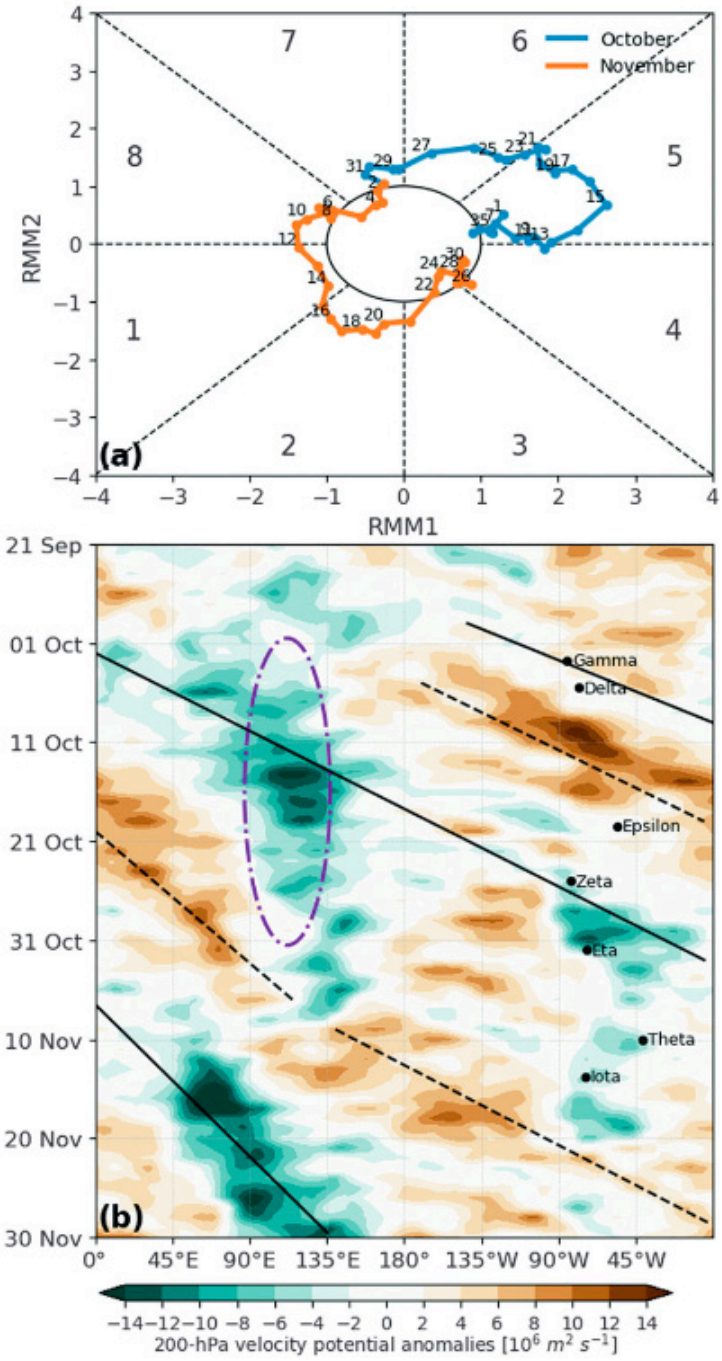

"(a) Propagation of the Madden-Julian oscillation during October-November 2020 according to the Wheeler and Hendon (2004) index. (b) Hovmöller diagram of Oct-Nov 200-hPa velocity potential anomalies spanning the globe averaged over 5°S-5°N. Convectively enhanced and convectively suppressed phases of the MJO are highlighted with solid and dashed lines, respectively. The relatively stationary enhancement of convection located around ~120°E is also highlighted with a dashed ellipse." Source: Klotzbach et al. 2022.

Figure 2. Madden-Julian oscillation during October-November 2020. Source: (Klotzbach et al. 2022).

A useful measure of individual and seasonal TC activity is furnished by the Accumulated Cyclone Energy (ACE). ACE is "defined as the sum of the squares of the maximum sustained surface wind speed (knots) measured every six hours for all named storms while they are at least tropical storm strength" (National Weather Service 2021). It is calculated as the square of the wind speed every six hours for the entire time that the cyclone is deemed a tropical storm (wind speed of at least 34 knots) and then scaled by a factor of 10^{-4} for usability with index values. We note for reference that ACE does not consider the size of the hurricane or tropical storm. The formula for calculating ACE is:

$$ACE = 10^{-4}\sum v^2 \tag{2}$$

Where v is the maximum sustained wind speed in knots and the unit for ACE being 10^4 kt^2. Hurricane Delta had an ACE of 15.7, ranking it as the fourth highest ACE of the 2020 Atlantic hurricane season. The ACE classification for a hurricane season's total activity is calculated by adding the ACE from all named storms. Table 1 shows NOAA's 2020 Atlantic hurricane season classifications of ACE (National Weather Service 2021). The ACE index for the 2020 hurricane season was, $180 \times 10^4\ kt^2$, making it extremely active.

Table 1. NOAA's Atlantic hurricane season classifications. Adapted from National Weather Service (2021).

Category	**ACE Index**	**Percent of 1951–2020 Median**
Extremely Active	Above $159.6 \times 10^4\ kt^2$	165%
Above-normal	Above $126.1 \times 10^4\ kt^2$	130%
Near-normal	73-$126.1 \times 10^4\ kt^2$	75-130%
Below-normal	Below $73 \times 10^4\ kt^2$	75%

An ongoing series of changes in the SSTs in the North Atlantic Ocean is the Atlantic multidecadal oscillation (AMO). The AMO has two phases, warm (positive) and cool (negative). These phases may last for 20–40 years with a difference of ~1°F between the

extremes. This oscillation is associated with changes in the frequency of severe Atlantic hurricanes. Warm phases are generally indicative of a greater number of tropical storms that mature to major hurricanes than that in cool phases. The last cool phase was from 1970–1994 and had an average of 1.5 major hurricanes per year in the Atlantic. Currently, the AMO is in a warm phase, which started in 1995, and from 1995–2020 there was an average of 3.6 major hurricanes per year. Comparing the last cool phase and the warm phase from 1995–2020, there is a noticeable difference in the increase of weak storms maturing into major hurricanes (NOAA AOML 2005).

Figure 3 shows that Oct-Nov 2020 had a pronounced interannual and multidecadal variability for hurricane activity relative to the period from 1950 to 2019. By focusing on ACE, we can highlight this variability. In Oct-Nov 2020 (red bar in Figure 3a) 74 x $10^4 kt^2$ of ACE was generated, making it the second highest ACE from 1950–2020. Figure 3a reveals also that Oct-Nov had a pronounced multidecadal variability in Atlantic hurricane activity. There is an increase in hurricane activity during 1950 to 1968 and 1995 to 2019 and a decrease in activity from 1970 to 1994. These multidecadal periods of high and low ACE correlate reasonably well with the AMO's positive and negative phases.

A positive AMO phase is associated with anomalously high tropical Atlantic SSTs, increased potential intensity (PI), and reduced vertical wind shear; these factors favor a more active Atlantic hurricane season. A negative AMO phase is associated with anomalously low North Atlantic SSTs, decreased PI, and increased vertical wind shear; these factors decrease the likelihood of an active Atlantic hurricane season (Kim et al. 2022).

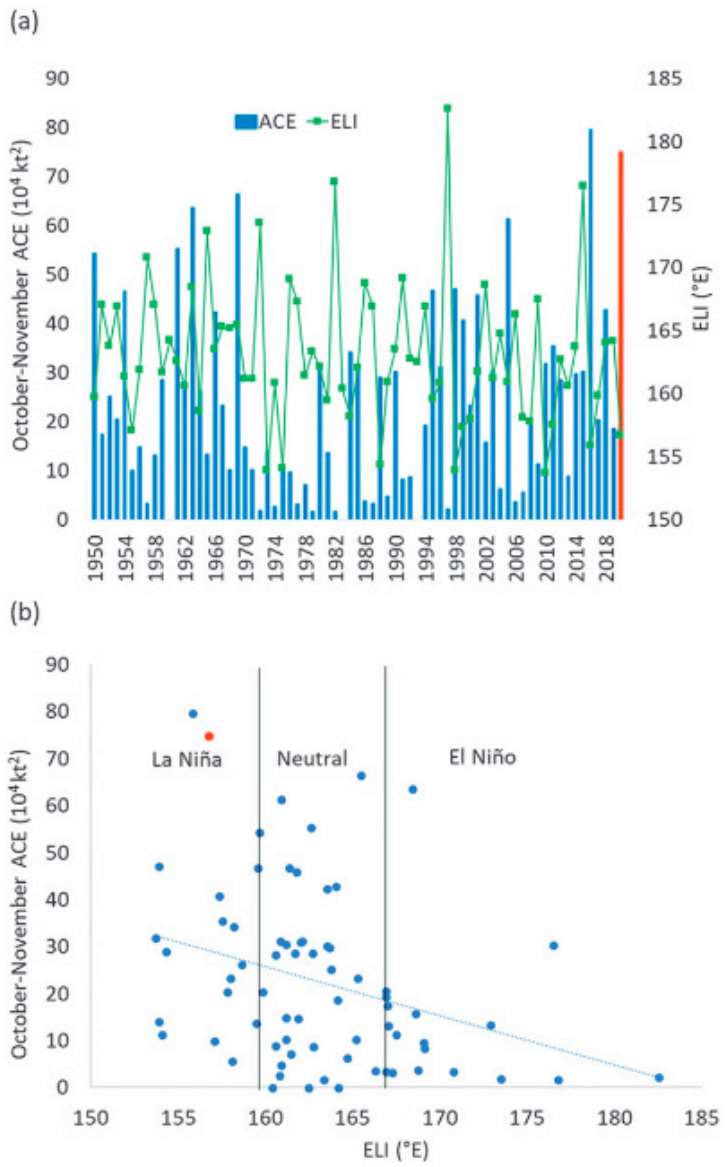

"(a) October–November Atlantic ACE from 1950 to 2020 (blue columns) and the ENSO longitude index (ELI) (green line). The red column highlights the observed ACE in October–November 2020. (b) Scatterplot of the relationship between October–November ACE and ENSO from 1950 to 2020 as represented by the ELI. The red dot represents the observed value of the ELI and October–November ACE in 2020, while the blue dashed line represents the regression relationship between the two time series from 1950 to 2019. Black lines delineate the longitude breakdowns between El Niño and neutral and neutral and La Niña conditions, respectively." Source: Klotzbach et al. (2022)

Figure 3. October-November 2020 Atlantic ACE. Source: (Klotzbach et al. 2022)

In October of 2020 the vertical wind shear, SST, relative humidity (RH), and PI were, overall, highly favorable in the Caribbean when compared to the past 42 years

(Figure 4). Here, PI is defined as "the maximum speed limit (upper bound) of a tropical cyclone found by modeling the storm as a thermal heat engine" (Gilford 2021) and follows the algorithm from Bister and Emanuel (2002). The equation used for PI is as follows:

$$(V_{max})^2 = \frac{C_k}{C_D} \frac{(T_s - T_0)}{T_0} (h_o^* - h^*) \quad (3)$$

In Equation 3, V_{max} is the maximum PI for a TC, C_k and C_D represent the enthalpy and momentum surface exchange coefficients, h_o^* is the sea surface saturation moist static energy, and h^* is the saturation moist static energy of air that is above the boundary layer and where the air above the boundary layer is generally evaluated at ~500-600 hPa (Gilford 2021). Using Equation 3 to predict the maximum gradient wind speed at the top of the frictional boundary layer, significant correlations can be seen between the PI and the actual wind speeds of storms. It has proven to be a useful zero-order diagnostic for evaluating and predicting TC intensity.

To explore the conditions in the Atlantic basin, the following subregional areas will be defined and highlighted; "western Caribbean as 10°–20°N, 84°–72°W; the eastern Caribbean as 10°–20°N, 72°–60°W; and the Gulf of Mexico as 20°–30°N, 97°–81° W" (Klotzbach et al. 2022). These areas can be seen highlighted by the orange boxes in Figure 4d.

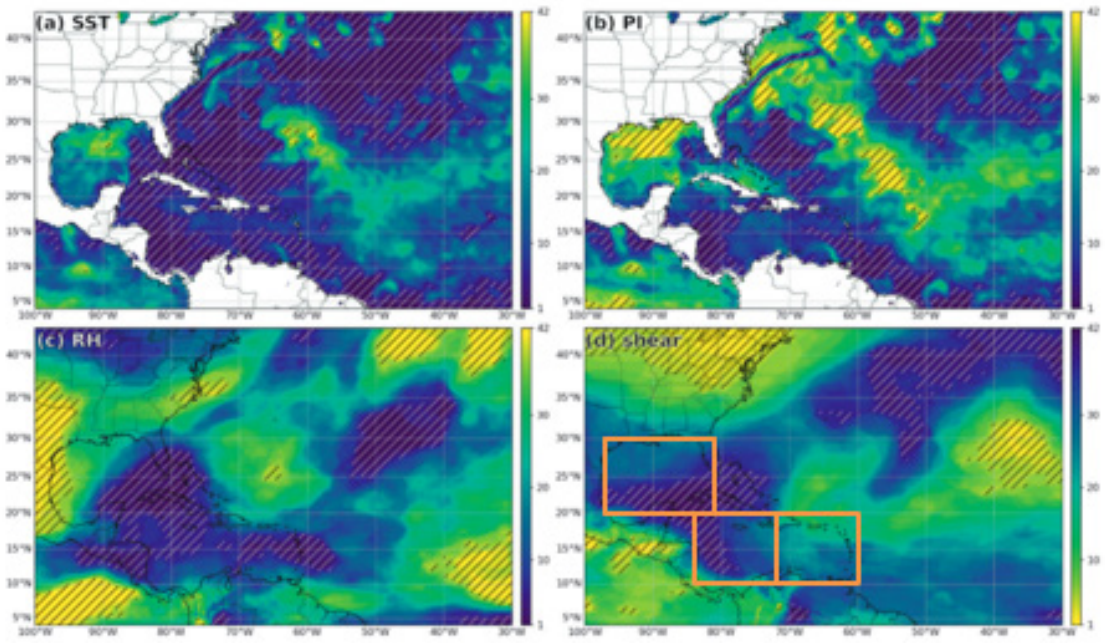

"Rank maps for October 2020 from ERA5 monthly averaged fields of (a) SST, (b) potential intensity, (c) 500–700-hPa relative humidity, and (d) 200–850-hPa wind shear. A rank of 1 represents the highest value during 1979–2020 and a rank of 42 the lowest. Purple shading indicates conditions more conducive for TCs; yellow shading indicates less conducive conditions. White hatching shows values that are in the top five most favorable for TCs, and black hatching shows values that are in the bottom five least favorable for TCs for each parameter." The three geographic regions mentioned in the paragraph above are represented by orange boxes in (d). Source: Klotzbach et al. (2022).

Figure 4. 2020 Rank Maps from ERA5. Source: (Klotzbach et al. 2022).

All four variables were conducive to TC formation for almost the entirety of the Caribbean in October 2020 (Figure 4). All AEWs first enter the Caribbean through the eastern Caribbean, which was characterized by the least favorable wind shear values (Figure 4d). That being said, the southern portion of the eastern Caribbean had weak vertical wind shear that may have allowed AEWs to reach the more favorable conditions in the western Caribbean where the SSTs, PI, RH, and vertical wind shear were all favorable for cyclogenesis. In contrast to the favorable conditions of the Caribbean, the Gulf of Mexico had somewhat cooler SSTs and lower PI. Nonetheless, the Gulf of Mexico still had relatively high RH and low vertical wind shear. It is thought by the authors of Klotzbach et al. that the cooler SSTs and lower PI contributed to the weakening of Hurricane Delta after entering the Gulf of Mexico, whereas the relatively high RH and low vertical wind shear contributed to the longevity of the TC.

THIS PAGE INTENTIONALLY LEFT BLANK

II. METHODOLOGY

A. MANUAL POUCH TRACKING USING THE GLOBAL FORECAST SYSTEM

At the Naval Postgraduate School, the Montgomery Research Group utilizes the MP conceptual framework and produces several quantitative products. These products are created using the Global Forecasting System (GFS) model outputs produced by the National Center for Environmental Prediction (NCEP) of the National Oceanic and Atmospheric Administration (NOAA) to analyze the model forecast. The method used generates images in the Earth-relative and co-moving frameworks. These images are used to identify the structural formation of wave pouches. In this thesis, the MP conceptual framework and analysis methodology are utilized with the goal of tracking the precursor pouch structure to its origin and gaining an understanding of the lifespan of the wave's pouch, the emergent proto vortex within it, and the subsequent consolidation and intensification of the vortex.

The process for tracking begins with the National Hurricane Center (NHC) Tropical Cyclone Report of Hurricane Delta to get the coordinates for when it was declared a tropical depression (TD). These coordinates are used as the initial point of our investigation. Additionally, the NHC Two-Day Graphical Tropical Weather Outlooks made prior to formation provide an estimated system velocity (wave phase speed) that was used to gain perspective on the zonal and meridional phase speeds for the co-moving framework. Using the estimated phase speeds, scripts written for the Grid Analysis and Display System (Center for Ocean-Land-Atmosphere Studies, Institute of Global Environment and Society, George Mason University) produced GFS analyses of the co-moving streamlines. These streamlines, along with the trough axis and critical latitude, were overlaid with the OW for the user to locate the pouch's position, which was then selected (Figure 5). This process is repeated in six-hour increments back in time at 00, 06, 12, and 18 UTC until the precursor was tracked to the coast of Africa. Careful and repeated examination of the analysis, especially before the NHC Two-Day Graphical Tropical Weather Outlook indicated a disturbance, allows for unique phase speeds to be assigned.

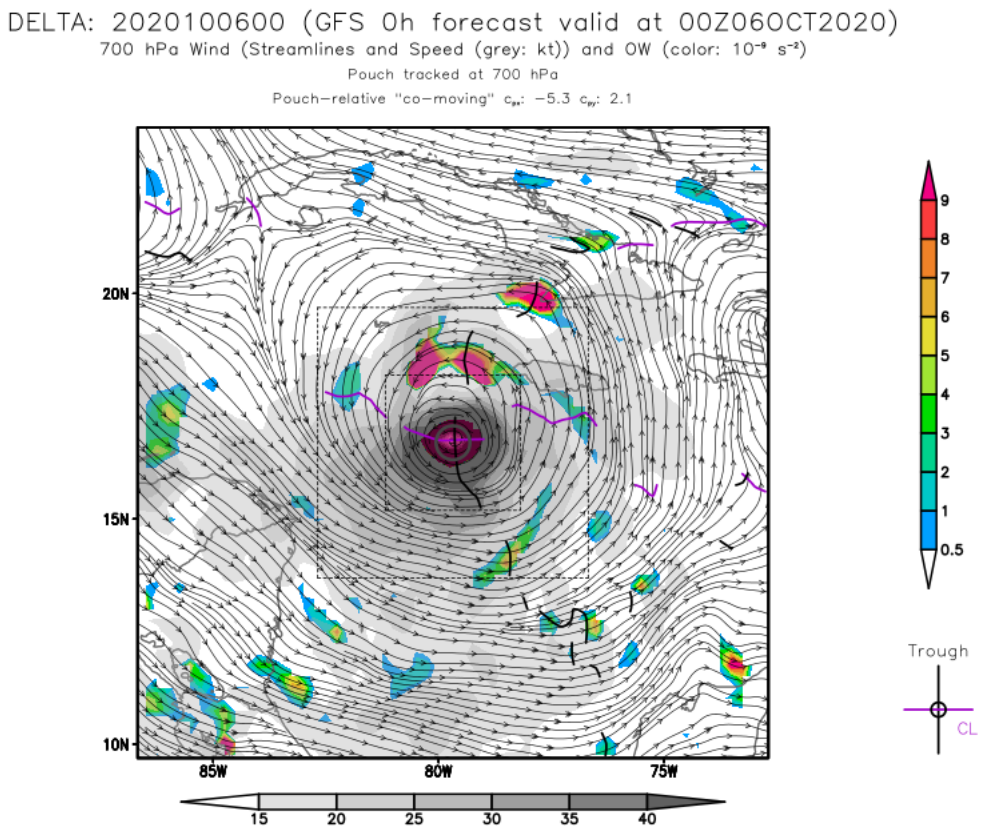

Depiction of the GFS analysis of OW (color shading) and co-moving streamlines and isotachs (grey shading) at 700 hPa for the NHC declaration of Hurricane Delta at 00 UTC 6 October 2020. The intersection of the trough axis (solid black line) and the critical latitude (solid purple line) marks the "sweet spot." Zonal and meridional phase speeds are westward at 5.3 m s^{-1} and northward at 2.1 m s^{-1}, respectively. Dashed lines depict 3°x3° and 6°x6° pouch-centered boxes. The concentric and closed streamlines surrounding the intersection are approximately collocated with the concentrated area of high OW values.

Figure 5. Depiction of the pouch at 700 hPa at 00 UTC 6 October 2020

This iterative process was repeated multiple times with careful analysis of the OW and relative vorticity at 700 hPa. In addition, 500 hPa and 850 hPa OW and relative vorticity fields were used to help refine the estimated phase speeds based on their locations using the Haversine formula. Locations and phase speeds were smoothed out to eliminate apparent discontinuities due to an inherent uncertainty of the center position. This inherent uncertainty occurs because pouches can be quite large geographically with multiple OW maxima. In view of these attributes, there is room for significant errors in phase speed calculations based on the selected center position. The smoothing allows for minimization of the impact from the significant errors that might occur in the overall analysis. While

tracking the AEW, there was a 24-hour time period when the early-stage precursor was weak with little to no circulation in the co-moving streamlines, but OW and relative vorticity organization were still evident. The center positions during that time have an additional uncertainty to them.

The output of the iterative analysis process produces horizontal cross section plots of OW, RH, relative vorticity, potential vorticity, horizontal wind direction and speed, and two forms ("deep" 200–850 hPa and a lower 500–850 hPa "pouch") of vertical wind shear. Additional diagnostic analyses include area averages of the variables calculated at multiple vertical levels for a 3°x3° horizontal box (approximately 207 km x 198 km) and for a 6°x6° horizontal box (approximately 414 km x 369 km) centered on the selected pouch location. Examples of a 3°x3° box and a 6°x6° box are shown in Figure 5. Each box has a different purpose; the 3°x3° box was used most frequently as it is focused on the interior region of the pouch, while the 6°x6° box was used only when required to identify specific larger-scale phenomena that typically include the pouch and its immediate surroundings. Synoptic scale products were also produced and analyzed for any large-scale interactions with Hurricane Deltas' pre-cursor, as seen in Figure 6. To create the time-height and time series plots that will be seen later in this study, a collection of the area-average outputs for the whole tracking period was used. Additionally, a stacked eight-panel image of 500 hPa, 700 hPa, 850hPa, and 925 hPa streamline fields in both co-moving and earth-relative frameworks is also produced to provide insight into the vertical structure of the candidate disturbance (Figure 7).

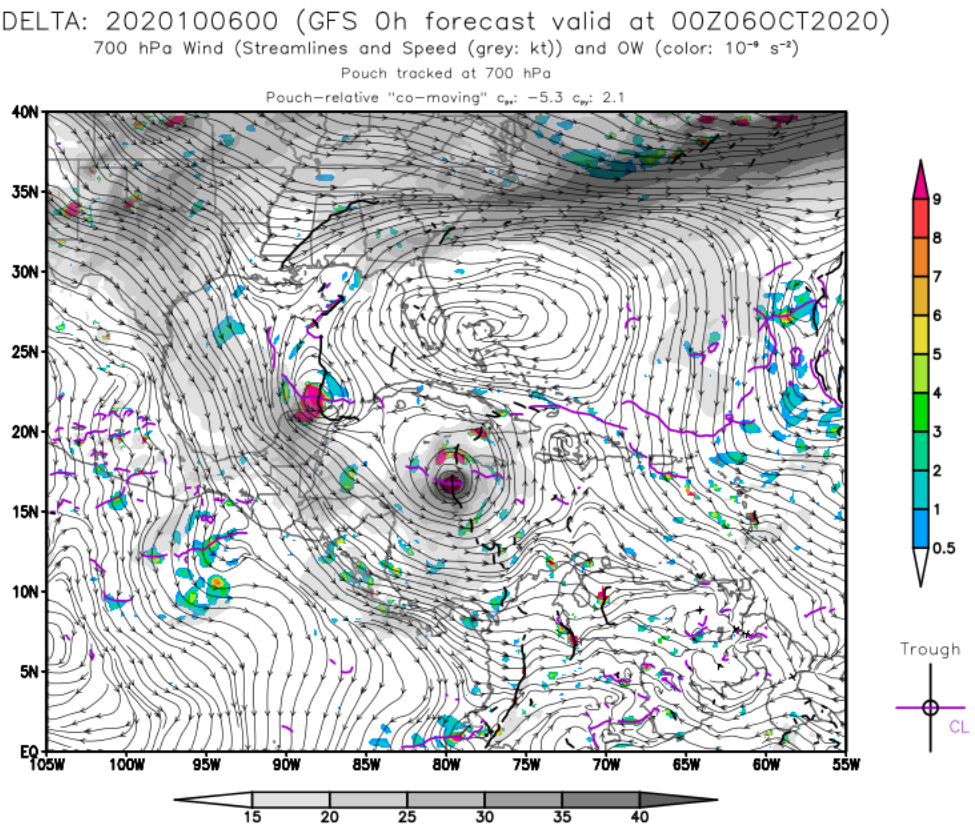

A large-scale depiction of the GFS analysis of OW (color shading) and co-moving streamlines and isotachs (grey shading) at 700 hPa when the NHC declared Hurricane Delta at 00 UTC 6 October 2020. Tropical storm Gamma is located at 21.9°N, 88.2°W according to the HNC, which is northwest of Hurricane Delta pouch tracked position of 16.7°N, 79.6°W.

Figure 6. Large scale depiction of the 700 hPa at 00 UTC 6 October 2020

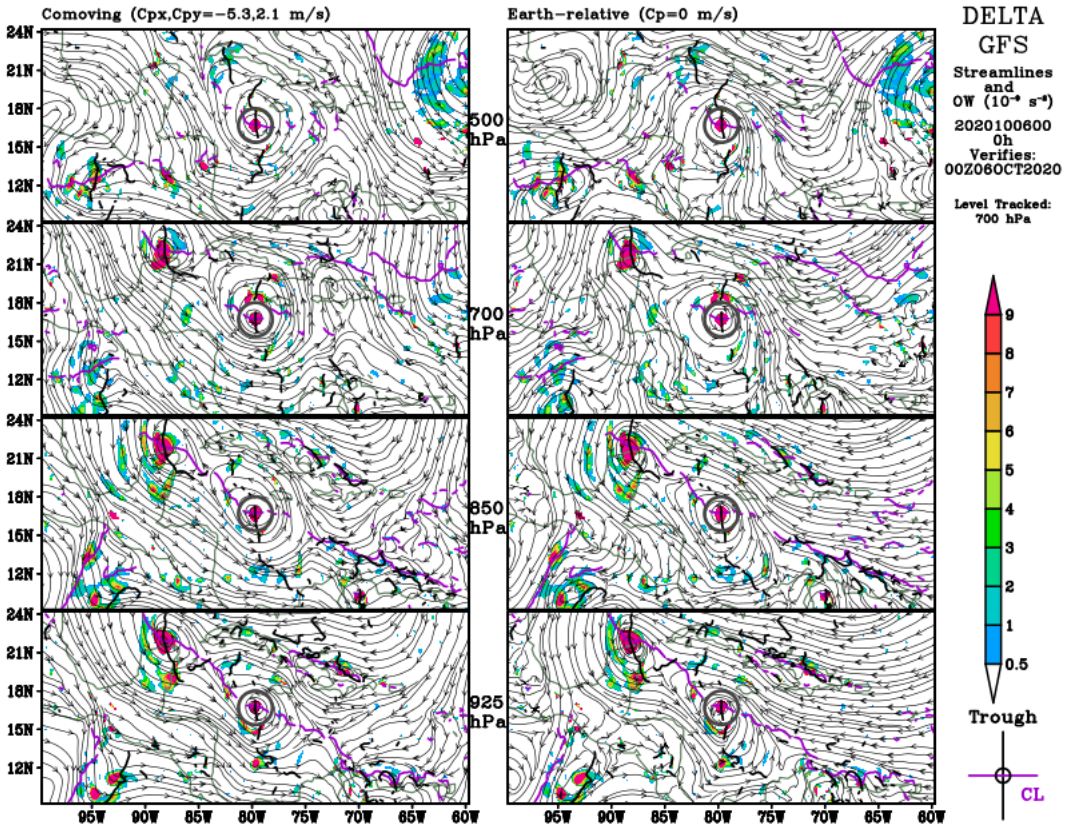

Eight-panel image of GFS OW overlaid by comoving (left) and Earth-relative (right) streamlines for 500, 700, 850, and 925 hPa (top to bottom) at 00 UTC 6 October 2020 when Delta was declared a hurricane by the NHC. It shows a closed circulation with an intersection of the critical latitude and trough in the center of the pouch in both the co-moving and Earth-relative frameworks.

Figure 7. 8-panel depiction of the pouch at 00 UTC 6 October 2020

As previously mentioned, two of the model outputs are deep and pouch vertical wind shear. The deep vertical wind shear is calculated by taking the magnitude of the difference between the horizontal winds at 850 and 200 hPa levels and averaging this difference over the 3°x3° or 6°x6° boxes. This calculation quantifies the upper-level jet and vertical wind shear effects present throughout the column of air. For the pouch vertical shear, the difference in horizontal winds between the 850 and 500 hPa are averaged over the 3°x3° or 6°x6° boxes. The pouch shear is more representative of the potential disruption to the vertical alignment of the pouch and the intrusion of environmental dry air over the vertical scale of the pouch.

B. SATELLITE IMAGERY

To observe the connection between the MP and reality, visible and infrared satellite images were retrieved from the NOAA National Centers for Environmental Information (NCEI) Comprehensive Large Array-Data Stewardship System (CLASS) to complement the model analyses. Satellite data were converted to WGS94 GeoTIFF format and then images were centered on pouch locations using Quantum Geographic Information System (GIS) software and the Geospatial Data Abstraction Library (Rouault et al. 2022) to allow easy comparison with the MP outputs, some of which are shown in this thesis. This process was focused on the six-hour increments mentioned previously (00, 06, 12, and 18 UTC) to corroborate the locations and magnitudes of dynamical features depicted by GFS with the convection in the satellite imagery. The Cloud and Moisture Imagery from the channel 13 clean longwave window on GOES-16 (formerly GOES-R before reaching geostationary orbit), provides cloud detection and heights, along with an insight to the intensity of hurricanes (Schmit et al. 2017). Channel 2 "red" visible images allows for daytime assessment of low-level clouds as well as overshooting tops of deep convection.

C. ADVANTAGES OF USING THE CO-MOVING FRAMEWORK

As previously mentioned, the key to the MP is the application of the co-moving framework, which applies the zonal and meridional phase speeds to the GFS model analysis and produces a more appropriate depiction of the atmospheric conditions relevant to a potential developing disturbance. As an example, Figures 8, 9, and 10, show that the streamlines in the Earth-relative framework are an open wave, while in the co-moving framework, the streamlines depict a closed circulation around the pouch's location. A common feature in Figures 8, 9, and 10 is that in the Earth-relative framework, there is a trough axis but no critical latitude, whereas in the co-moving framework, the trough axis and critical latitude intersect.

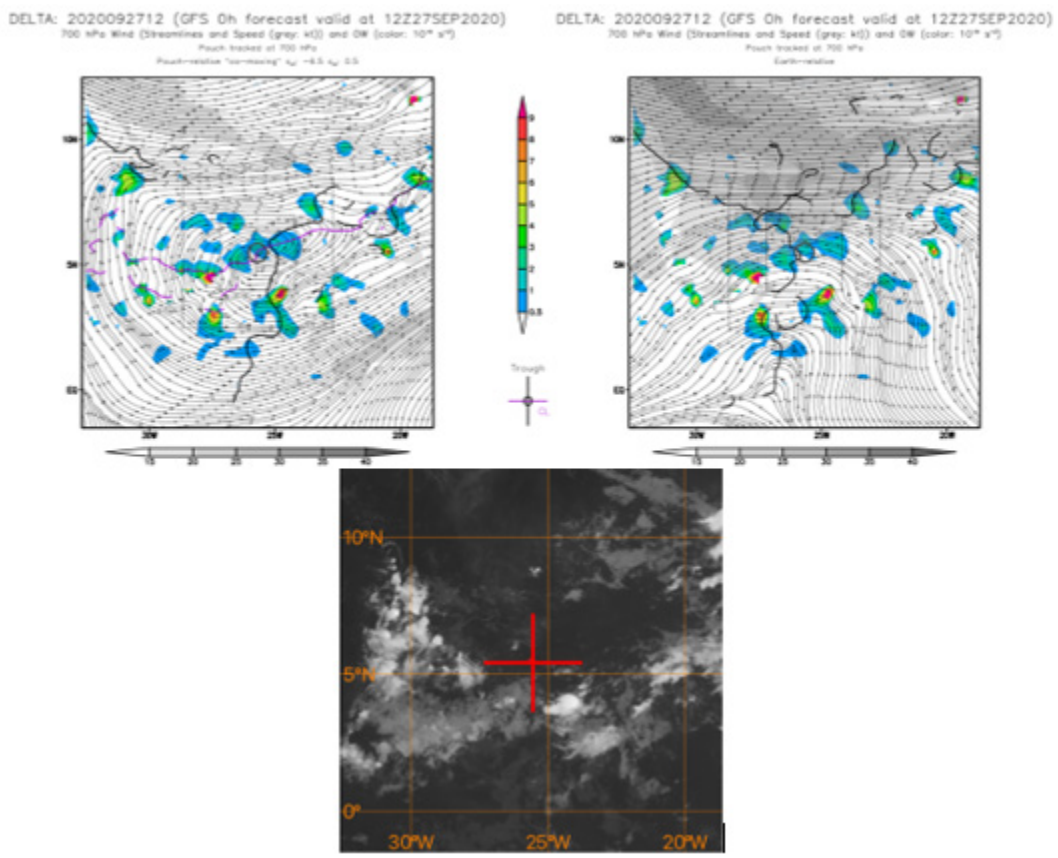

GFS analysis of 700 hPa OW at 12 UTC 27 September 2020 with 700 hPa streamlines in the co-moving (top left) and Earth-relative (top right) frameworks, with the 700 hPa tracked position denoted by a circle. GOES infrared (IR) image (bottom center) indicates the pouch's location by the red cross. The co-moving framework shows a closed circulation in the form of an ellipse surrounding the pouch's location. In the Earth-relative framework there is an open wave.

Figure 8. GFS analysis of OW in co-moving and Earth-relative frameworks with GOES IR satellite imagery at 12 UTC 27 September 2020

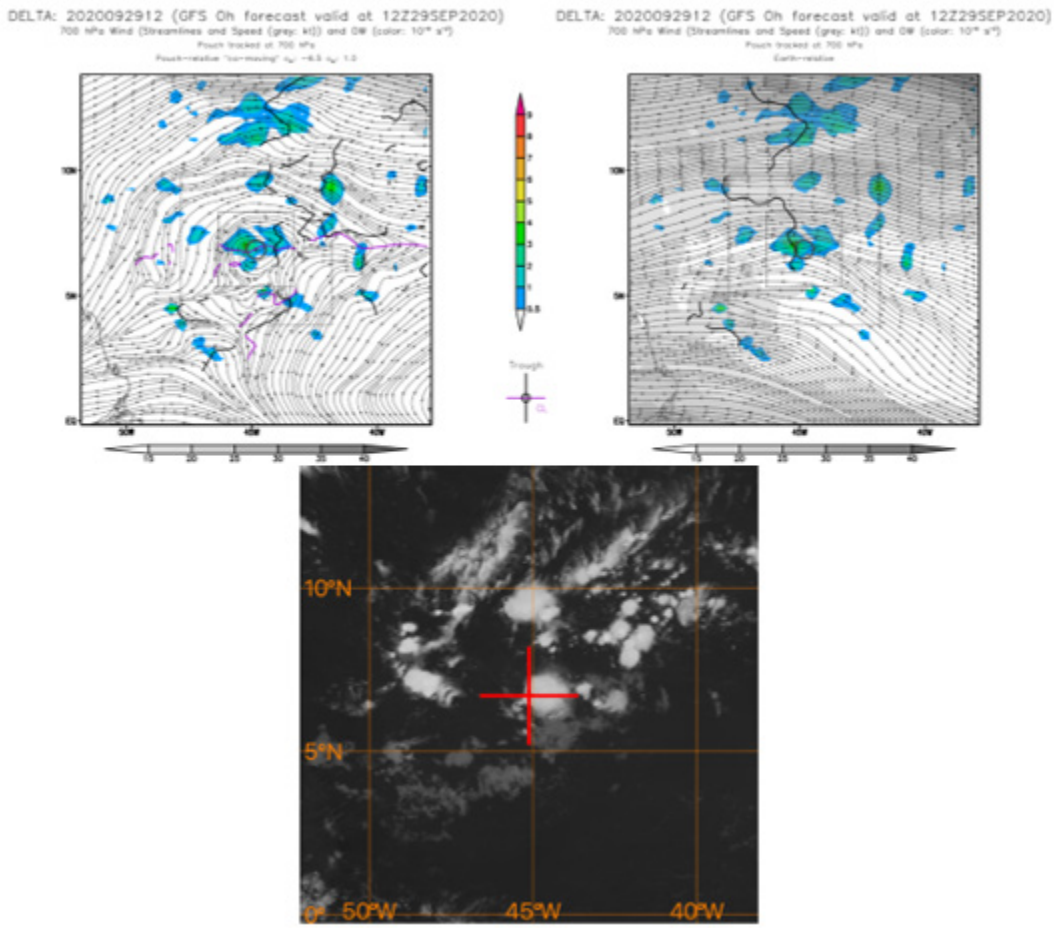

GFS analysis of 700 hPa OW at 12 UTC 29 September 2020 with 700 hPa streamlines in the co-moving (top left) and Earth-relative (top right) frameworks, with the 700 hPa tracked position denoted by a circle. GOES infrared (IR) image (bottom center) indicates the pouch's location by the red cross. The co-moving framework shows a closed circulation in the form of an ellipse surrounding the pouch's location. In the Earth-relative framework there is an open wave.

Figure 9. GFS analysis of OW in co-moving and Earth-relative frameworks with GOES IR satellite imagery at 12 UTC 29 September 2020

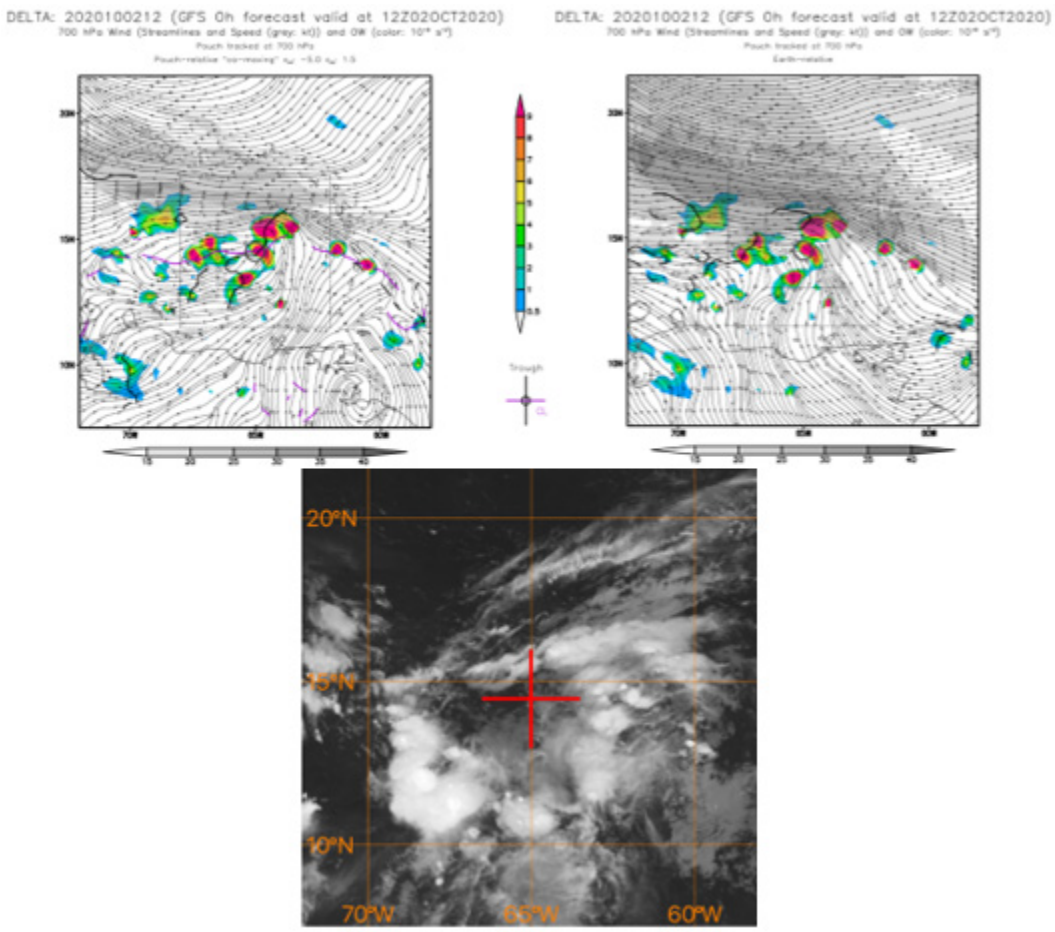

GFS analysis of 700 hPa OW at 12 UTC 2 October 2020 with 700 hPa streamlines in the co-moving (top left) and Earth-relative (top right) frameworks, with the 700 hPa tracked position denoted by a circle. GOES infrared (IR) image (bottom center) indicates the pouch's location by the red cross. The co-moving framework shows a closed circulation in the shape of an ellipse and in the Earth-relative framework there is no closed circulation.

Figure 10. GFS analysis of OW in co-moving and Earth-relative frameworks with GOES IR satellite imagery at 12 UTC 2 October 2020

It is clear from Figures 8, 9, and 10 that the co-moving framework shows a closed circulation as the pouch traverses the Atlantic Ocean into the Caribbean Sea, whereas the Earth-relative framework shows an open wave. The Earth-relative framework begins to show a quasi-closed circulation at 12 UTC 2 October, but does not show a well-defined closed circulation until 18 UTC on 4 October. It is at this time that the NHC declared AL262020 a TD, as seen in Figure 11.

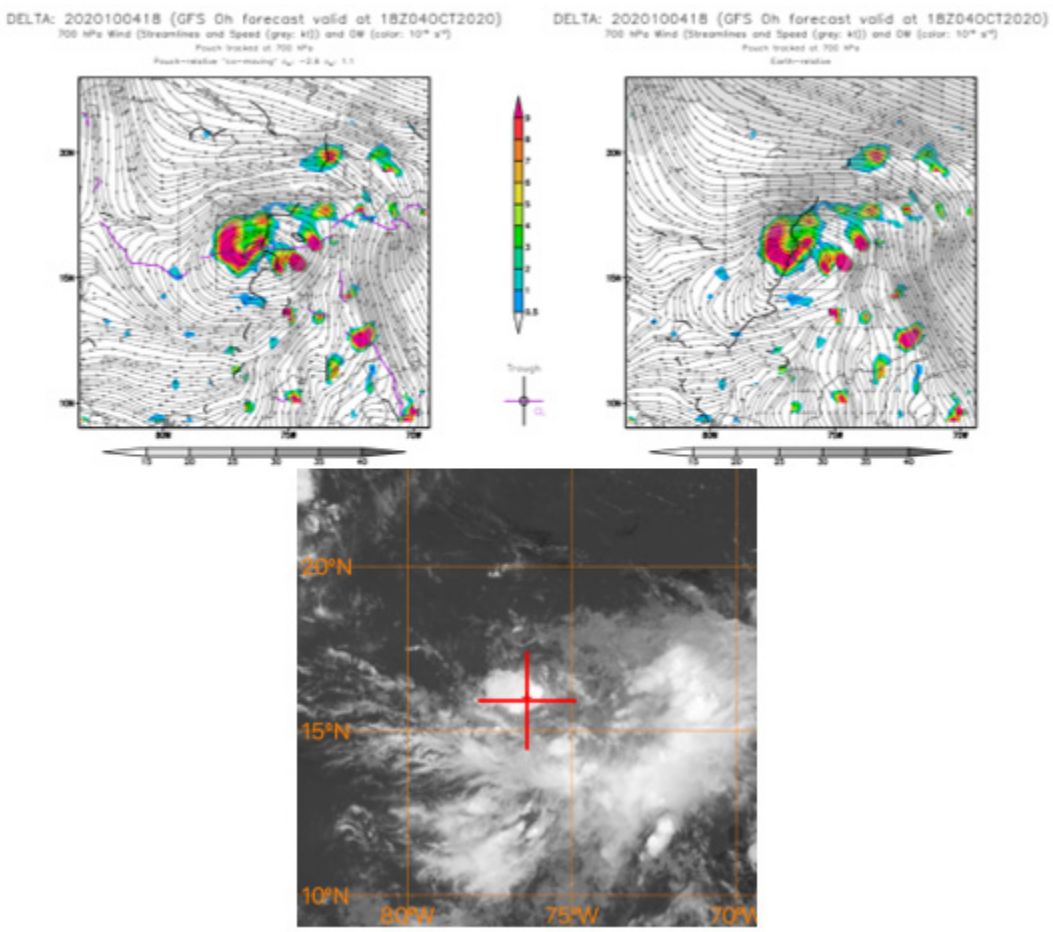

GFS analysis of 700 hPa OW at 18 UTC 4 October 2020 with 700 hPa streamlines in the co-moving (top left) and Earth-relative (top right) frameworks, with the 700 hPa tracked position denoted by a circle. GOES infrared (IR) image (bottom center) indicates the pouch's location by the red cross. This is first time both frameworks show a closed circulation and when the NHC declared AL262020 a tropical depression.

Figure 11. GFS analysis of OW in co-moving and Earth-relative frameworks with GOES IR satellite imagery at 18 UTC 4 October 2020

By viewing streamlines in a co-moving framework, the structure of the recirculating airflow, the formation of a proto vortex and its subsequent modification by diabatic vortices, the evolution of moist entropy, moist potential vorticity and other adiabatic invariants in and around the recirculating region can be meaningfully visualized (Dunkerton et al. 2009).

III. RESULTS

This chapter will focus on the results of the research of the MP as it pertains to Hurricane Delta. There are three areas of interest in this chapter to give a more in-depth look into the genesis and lifespan of Delta. The three areas of interest are: the association of the pre-Delta pouch with convection, the stalling and alignment period of the pre-Delta disturbance, and the rapid intensifications (RI) periods that occurred once the disturbance was identified as a TD by NHC forecasters. This chapter will include additional information from the area-averaged time-series and time height plots introduced in Chapter II, as well as the two landfall events.

The deep convection near and within the pre-Delta pouch is a section which notes the importance of recognizing that not all convection from AEWs is associated with pouches, but pouches are always associated with convection near and within pouches. The stalling and alignment period of the pre-Delta pouch emphasizes the importance of synoptic scale effects on pouches and the necessity for vertical alignment, especially in the lower levels, for cyclogenesis. With the RI of Hurricane Delta being one for the record books of hurricane intensifications, it is important to identify the factors that played into the intensification, along with its following rapid weakening. The upcoming sections take a closer look at these three different periods of the disturbance/storm life cycle. Figure 12 highlights these events in a simple timeline.

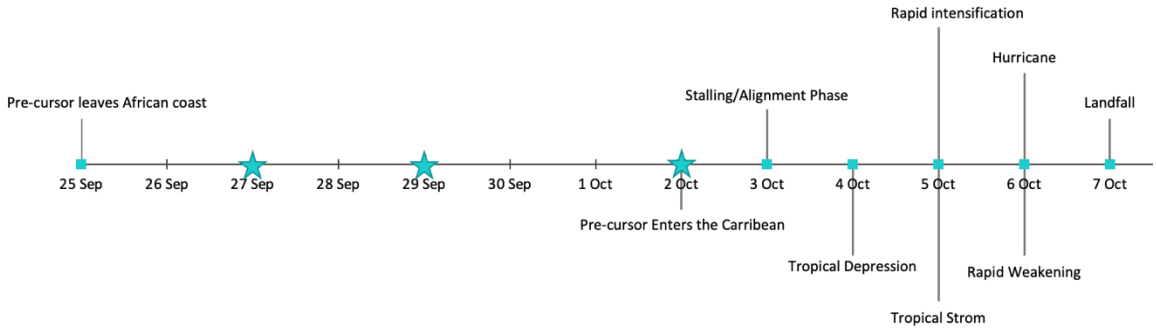

A timeline schematic of Hurricane Delta with the three areas of interest and the declaration of tropical depression, tropical storm, and Hurricane Delta. The blue stars indicate times that are featured in the discussion of deep convection near and within the pre-Delta pouch.

Figure 12. Timeline schematic of Hurricane Delta to first landfall

A. DEEP CONVECTION NEAR AND WITHIN THE PRE-DELTA POUCH

In Figure 13 IR satellite images with NHC enhancement highlight the precursor storm features every two or three days at 12 UTC from 26 September 2020 to 7 October 2020. These NHC enhancement images are shown on a map of the Atlantic Basin providing a visual aid of the pre-Delta disturbance track. The color scale on the right-hand side of Figure 13 identifies the presence of clouds. Warmer colors (colder temperatures) indicate higher cloud tops and cooler colors (warmer temperatures) indicate low to no cloud tops.

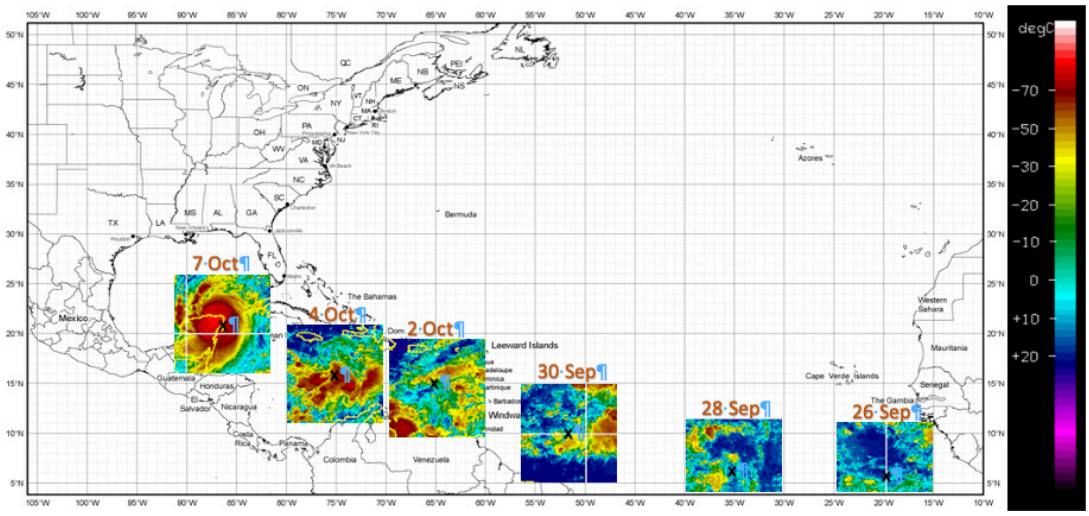

Infrared satellite images with NHC enhancement at 12 UTC on particular days from 26 September to 7 October 2020, showing the track of Delta's precursor coming off the African coast and continuing into the Caribbean Sea, which later became a hurricane on 6 October 2020. The black "x" on each NHC enhanced image is the approximate location of marsupial paradigm of the pre-Delta storm and the center of the storm after storm declaration by NHC forecasters. To the right of the Atlantic Basin map is the temperature in degrees Celsius. Sources: (NHC) and (University of Wisconsin – CIMSS).

Figure 13. GOES IR satellite imagery with NHC enhancement track of pre- and named Hurricane Delta

Starting at 12 UTC 26 September 2020, the image shows that there are low to midlevel clouds in the area surrounding the center of the image (the pouch's approximate location). As time passes and the pouch crosses the Atlantic Ocean, the images show a progressive increase in cloud coverage with higher cloud tops. After entering the Caribbean Sea, the images show that high cloud tops are in close proximity to the pouch's location. As seen in Figure 13, the pouch has clouds, otherwise known as convection, in the area surrounding it. Later, the convection is drawn towards the pouch center and becomes the focal point of the developing system.

Taking a closer look at Delta's precursor disturbance traveling westward across the Atlantic Ocean and into the Caribbean Sea, there were several instances when convection was in the vicinity of the sweet spot, but not coincident with its location. In Figures 14, 15, and 16 the OW, relative vorticity, and GOES-16 IR satellite imagery with georeferencing are used to compare the pouch's location with the satellite images for convection in a

14°x14° box. Figures 14, 15, and 16 depict three instances where scattered convection was in the surrounding area but not centered at the sweet spot.

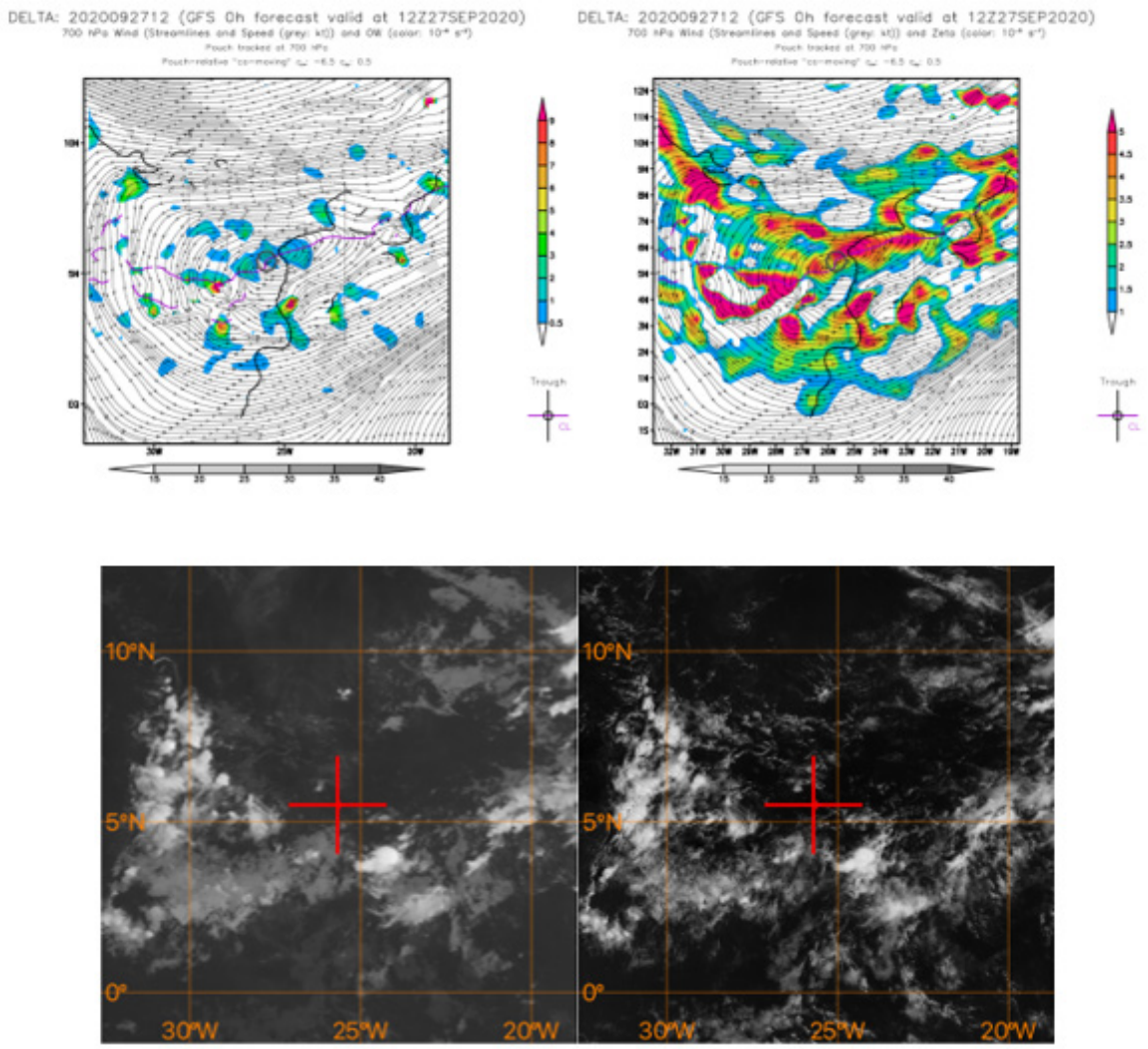

GFS analysis of OW (top left) and relative vorticity (top right) with 700 hPa streamlines in the co-moving framework at 12 UTC 27 September 2020 with the precursor moving at 6.5 m s^{-1} westward and 0.5 m s^{-1} northward. The units for OW are × 10^{-9} s^{-2}, and the units for relative vorticity are × 10^{-5} s^{-1}. The IR satellite (bottom left) and visible satellite (bottom right) imagery show convection around the pouch's location (red crosshair).

Figure 14. Convection surrounding the pouch at 12 UTC 27 September 2020

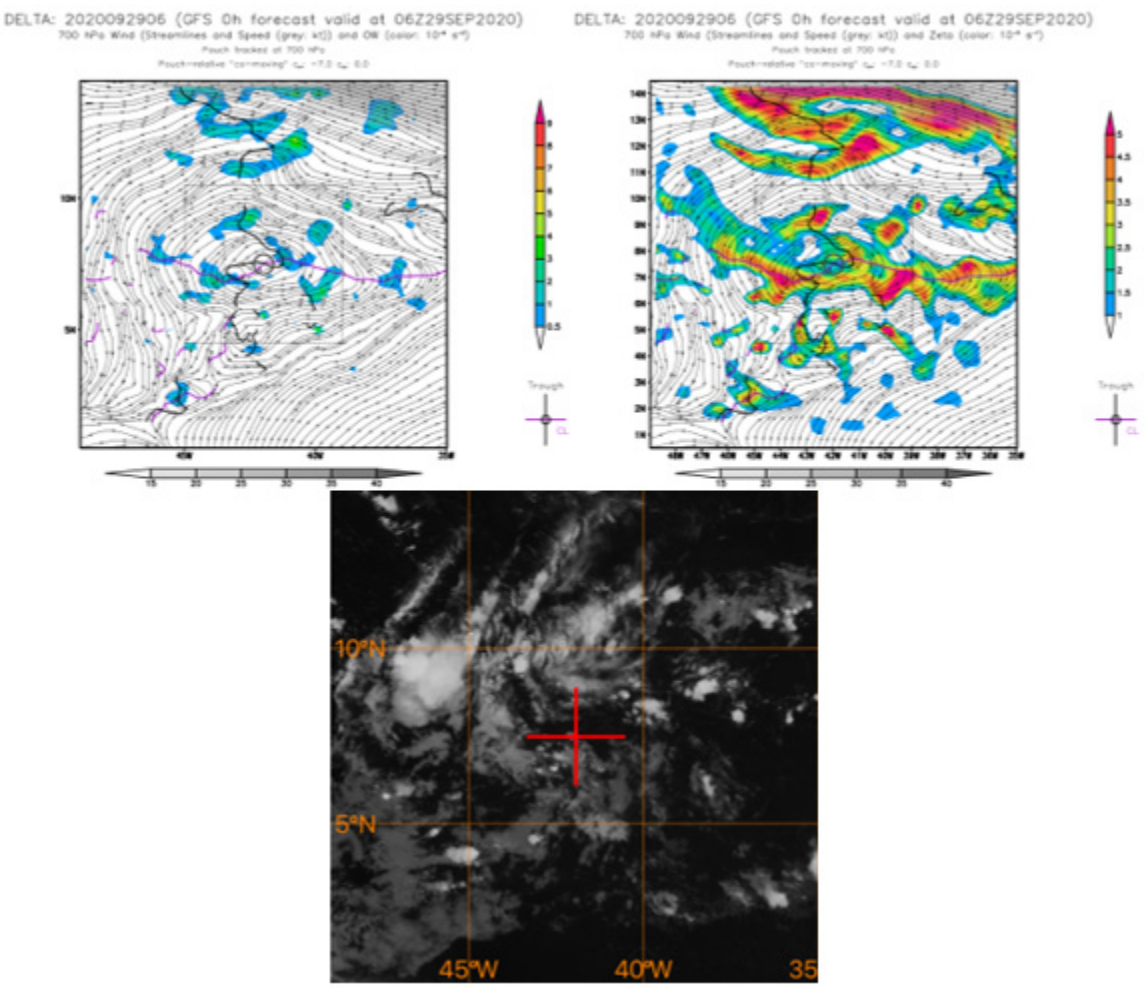

GFS analysis of OW (top left) and relative vorticity (top right) with 700 hPa streamlines in the co-moving framework at 06 UTC 29 September 2020 with the precursor moving at 7.0 m s^{-1} westward and 0.0 m s^{-1} northward. The units for OW are × 10–^{9} s^{-2}, and the units for relative vorticity are × 10–^{5} s^{-1}. The IR satellite (bottom center) shows convection around the pouch's location (red crosshair). There is no visible satellite imagery for this time.

Figure 15. Convection surrounding the pouch at 06 UTC 29 September 2020

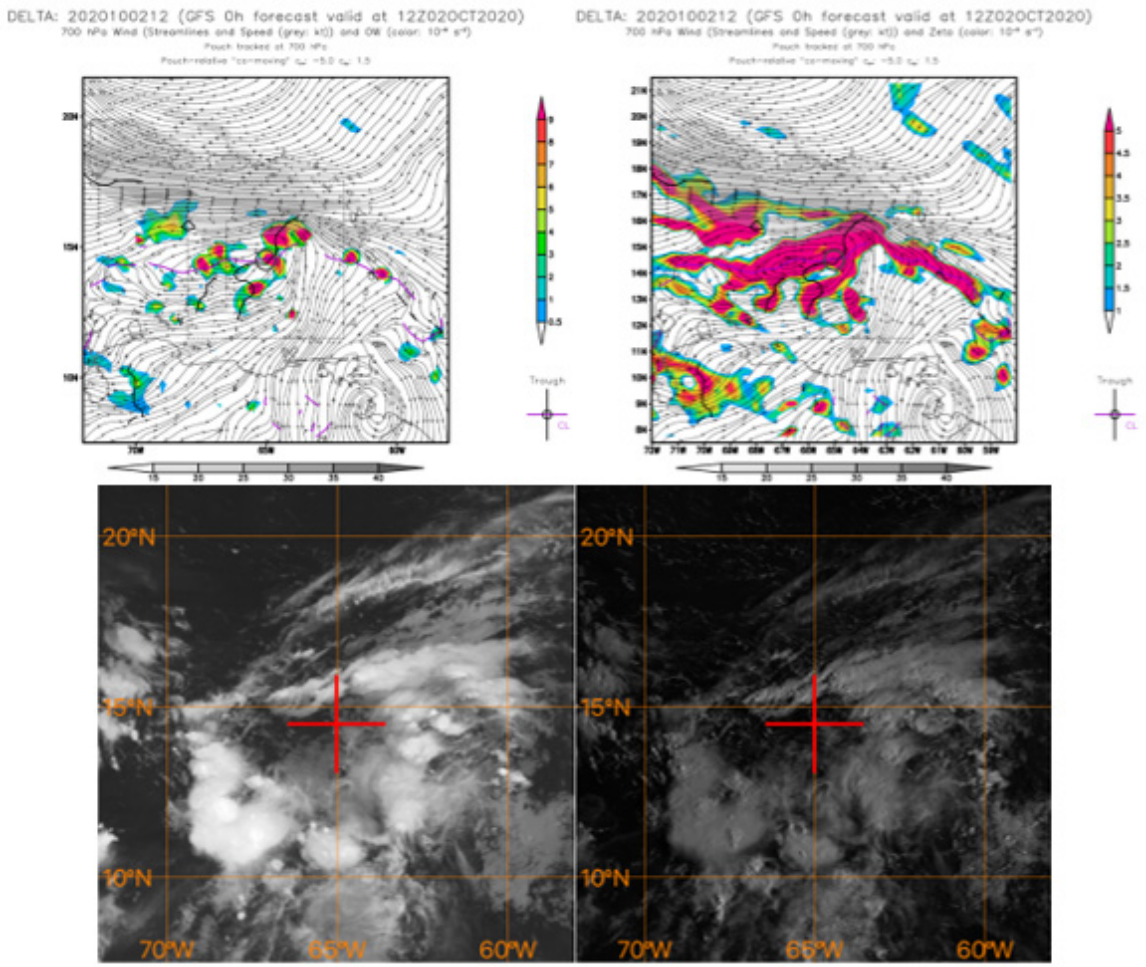

GFS analysis of OW (top left) and relative vorticity (top right) with 700 hPa streamlines in the co-moving framework at 12 UTC 2 October 2020 with the precursor moving at 5.0 m s^{-1} westward and 1.5 m s^{-1} northward. The units for OW are $\times 10^{-9}$ s^{-2}, and the units for relative vorticity are $\times 10^{-5}$ s^{-1}. The IR satellite (bottom left) and visible satellite (bottom right) imagery show convection around the pouch's location (red crosshair).

Figure 16. Convection surrounding the pouch at 12 UTC 2 October 2020

From Figures 14, 15, and 16, we can observe the convection encompassing the sweet spot's location over time. At first, the convection is located to the south and west of the pouch, and as time progresses, the convection moves to the north and northwest of the pouch. In Figure 16, the convection has surrounded the pouch.

B. STALLING/ALIGNMENT PHASE

A stalling phase occurred from approximately 00 UTC 3 October 2020 to 00 UTC 4 October 2020 (Figure 17). The stalling is thought to be due to a weakening of steering

flow in association with the rapid intensification (RI) of AL252020 into Hurricane Gamma. This RI was associated with a local high-pressure anomaly immediately to the east of the system. This high-pressure anomaly is likely associated with the generation of a Rossby wave wake behind the intense vortex of Hurricane Gamma during this time (McWilliams and Flierl 1979), which was also superimposed with the nearby Bermuda High. Support for this interpretation is as follows. The RI of AL252020 started from approximately 18 UTC 2 October 2020 to 1645 UTC 3 October 2020, with a 30-kt wind increase, forming a peripheral ridge that slowed the phase speed of AL262020's pouch. This ridge, paired with the Bermuda High (Figure 18), contributed to the precursor slowing and shifting from a west-northwest path to a west-southwest path.

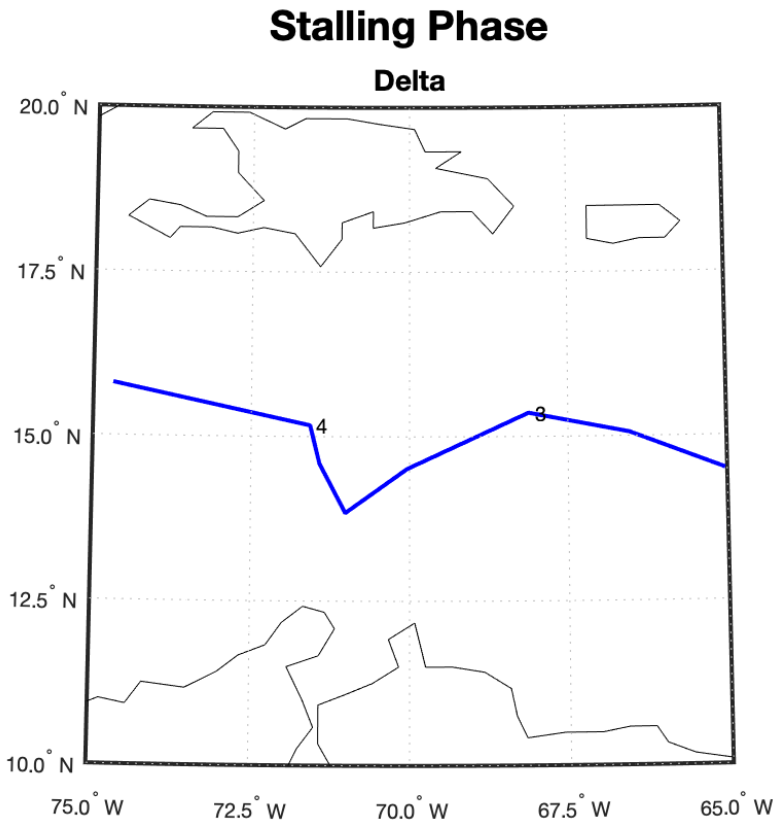

Pouch track (blue line) at 700 hPa from approximately 12 UTC 2 October to 06 UTC 4 October with 00 UTC 3 October 2020 and 00 UTC 4 October 2020 numbered on the track. As the tropical storm AL252020 intensified into Hurricane Gamma, a peripheral ridge formed, stalling Delta's precursor between 67.5°-72.0°W and 13.0°-16.0°N for approximately 24 hours. This time frame correlates with the amount of time AL252020 took to intensify and become a hurricane.

Figure 17. Track of pre-cursor Delta stalling phase

The stalling phase enabled the tilted pouch system to come into better vertical alignment for cyclogenesis. With the subsequent weakening of Hurricane Gamma to a tropical storm (TS) after landfall at approximately 1645 UTC 3 October 2020, the peripheral ridge weakened and allowed for AL262020's vertically aligned pouch to continue in the Caribbean Sea, where the SST, PI, RH, and vertical wind shear became progressively more favorable on its course to the Yucatan Peninsula.

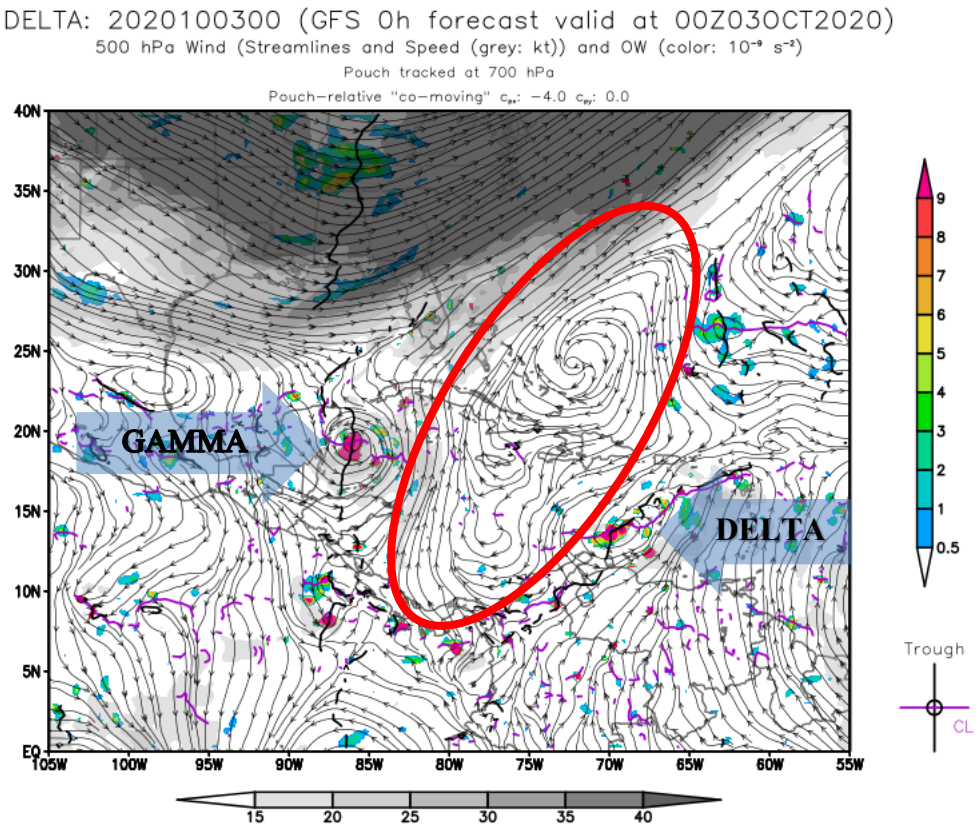

GFS analysis of streamlines, wind speeds (gray shading), and OW (color shading) at 500 hPa at 00 UTC 3 October 2020 that depicts the Delta precursor's comoving frame of the Caribbean Sea. Here, the anticyclonic flow from the Rossby wave wake and the superimposed Bermuda High is annotated by the red oval. Intensifying Hurricane Gamma is to the west of the oval while AL262020, Delta's precursor, is to the east.

Figure 18. GFS Analysis of OW at 500 hPa during the stalling/alignment phase

The alignment process is suggested by a diagnostic analysis using the pouch products. In Figure 19 the GFS analysis shows the "sweet spot" of AL252020, which intensified and became Hurricane Gamma at 1645 UTC 3 October 2020. The grey circle in each image indicates the location of the pouch for AL262020, which develops into Hurricane Delta. The left column of Figure 19 depicts the co-moving frame at 18 UTC 2 October 2020, approximately eight hours before the RI of AL252020 commenced. The left panel shows AL262020 to have a closed circulation with a positive OW feature at 700 hPa with weak OW outside of the grey circle. The 500 hPa level has a closed circulation, with only scattered regions of positive OW on its western, southern, and eastern periphery. The

850 hPa and the 925 hPa levels each have OW maxima on the northern portion of the grey circle and are indicated by the red arrows. These locations of OW indicate that there is a moderate southward tilt in the vertical.

The right panel of Figure 19 depicts the co-moving frame at 18 UTC 3 October 2020, when Hurricane Gamma had weakened and declared a TS. There is a closed circulation for AL262020 at the pouch location from 500 hPa to 850 hPa with strong OW in the area. At the 925 hPa level, there is a closed circulation with moderate to weak OW to the west-southwest of the pouch's 700 hPa location. From the OW fields and diagnosed "sweet spot," a slight eastward tilt is evident between the 500 hPa and 850 hPa levels, but it has become more vertically aligned than in the previous 24 hours. The 925 hPa level does not have a strong OW presence at this time nor a closed circulation at the pouch's location. However, both the 850 hPa and 925 hPa levels have a closed circulation with an OW maximum and sweet spot to the west-southwest, with an intersection of the critical latitude and trough axis indicated by the blue arrows.

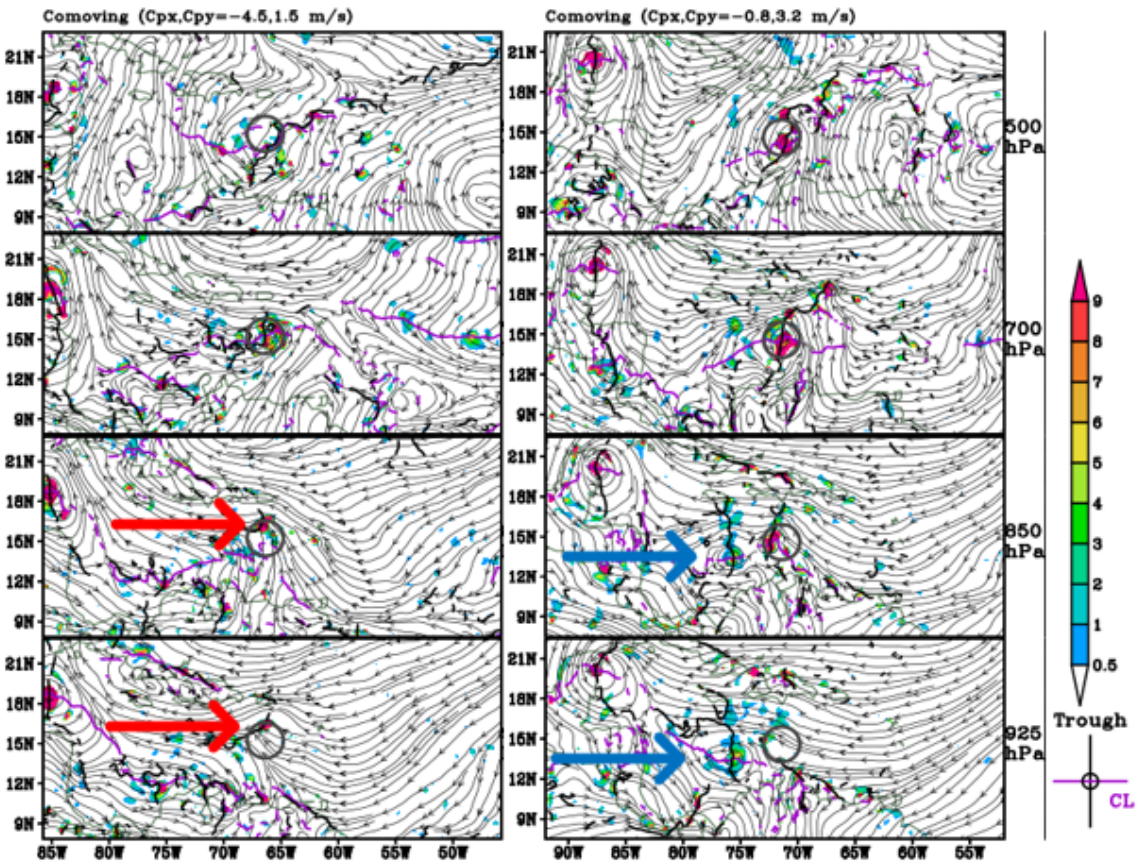

8-Panel comparison in the co-moving framework of streamlines and OW ($\times 10^{-9}$ s^{-2}) with the pouch tracked at 700 hPa on 18 UTC 2 October 2020 (left) and 18 UTC 3 October 2020 (right). The pouch "sweet spot" that is in the upper left of each pressure level is a tropical storm (TS), identified as AL252020 by the NHC, which would intensify to Hurricane Gamma at 1645 UTC 3 October 2020. The red arrows indicate the OW maximum at the 925 and 850 hPa levels on 18 UTC 2 October 2020 and the blue arrows indicate the OW maximum that is to the west-southwest of the sweet spot location at 700 hPa on 3 October 2020. The OW values have been multiplied by 10^9 for plotting purposes.

Figure 19. 8-Panel comparison of the start and end of stalling

While the stalling of Delta's pre-cursor allowed for the alignment of the 500 and 700 hPa levels, for a hurricane to develop, there needs to be an alignment of all pressure levels. Figure 20 shows that after the stalling phase the low-level (850and 925 hPa) OW maxima, which were west-southwest of the 700 hPa pouch location, began to weaken and be absorbed by the intensifying 700-hPa circulation. At 00 UTC 4 October 2020 (Figure 20, left), the 850 hPa sweet spot is nearly in vertical alignment with the 500 and 700 hPa

sweet spots. By 12 UTC 4 October 2020 (Figure 20, right), the sweet spots on all four levels were vertically aligned. After six hours of full vertical alignment, the system was declared a TD at 18 UTC 4 October 2020. This final absorption and deepening of the vertical alignment took approximately 24 hours to culminate in the official formation of TD26L, which would then intensify into TS Delta at 12 UTC 5 October.

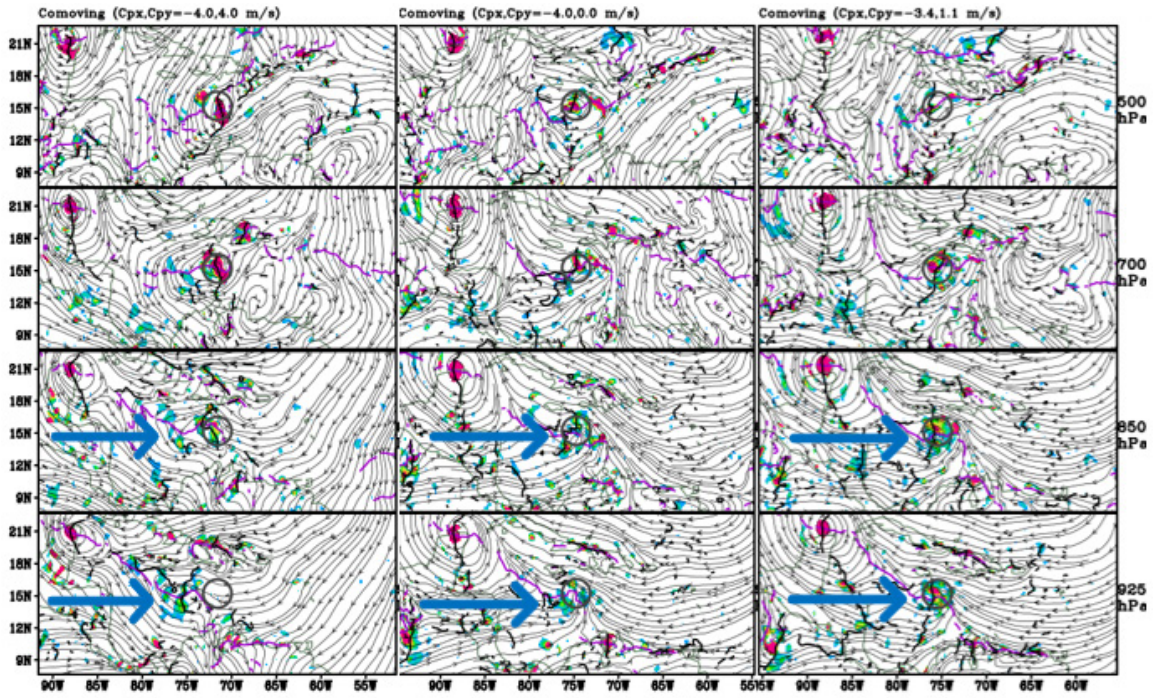

12-Panel comparison in the co-moving framework of streamlines and OW ($\times 10^{-9}$ s^{-2}) with the pouch tracked at 700 hPa on 00 UTC 4 October 2020 (left), 06 UTC 4 October 2020 (center), and 12 UTC 4 October 2020 (right). The blue arrow follows the OW maximum west-southwest of the tracked 700 hPa pouch as it comes into vertical alignment with the system of pre-cursor Delta.

Figure 20. 12-Panel of the full alignment of pre-cursor Delta

C. RAPID INTENSIFICATION

Hurricane Delta underwent two rapid intensification (RI) phases and one rapid weakening phase. The first RI began at approximately 06 UTC 5 October and ceased at 1800 UTC 6 October, during which wind speeds increased by 90 kts. Delta attained a maximum sustained winds of 120kts, making it a category 4 hurricane on the Saffir Simpson scale (Cangialosi and Berg 2021). Only four other Atlantic tropical cyclones have

had such an intensification rate or greater during the satellite era of over 60 years (Cangialosi and Berg 2021). This RI resulted in a pinhole eye (Figure 21) which was circular, surrounded by deep convection, with a diameter of four nautical miles at 1633 UTC 6 October 2020 (Tropical Atlantic).

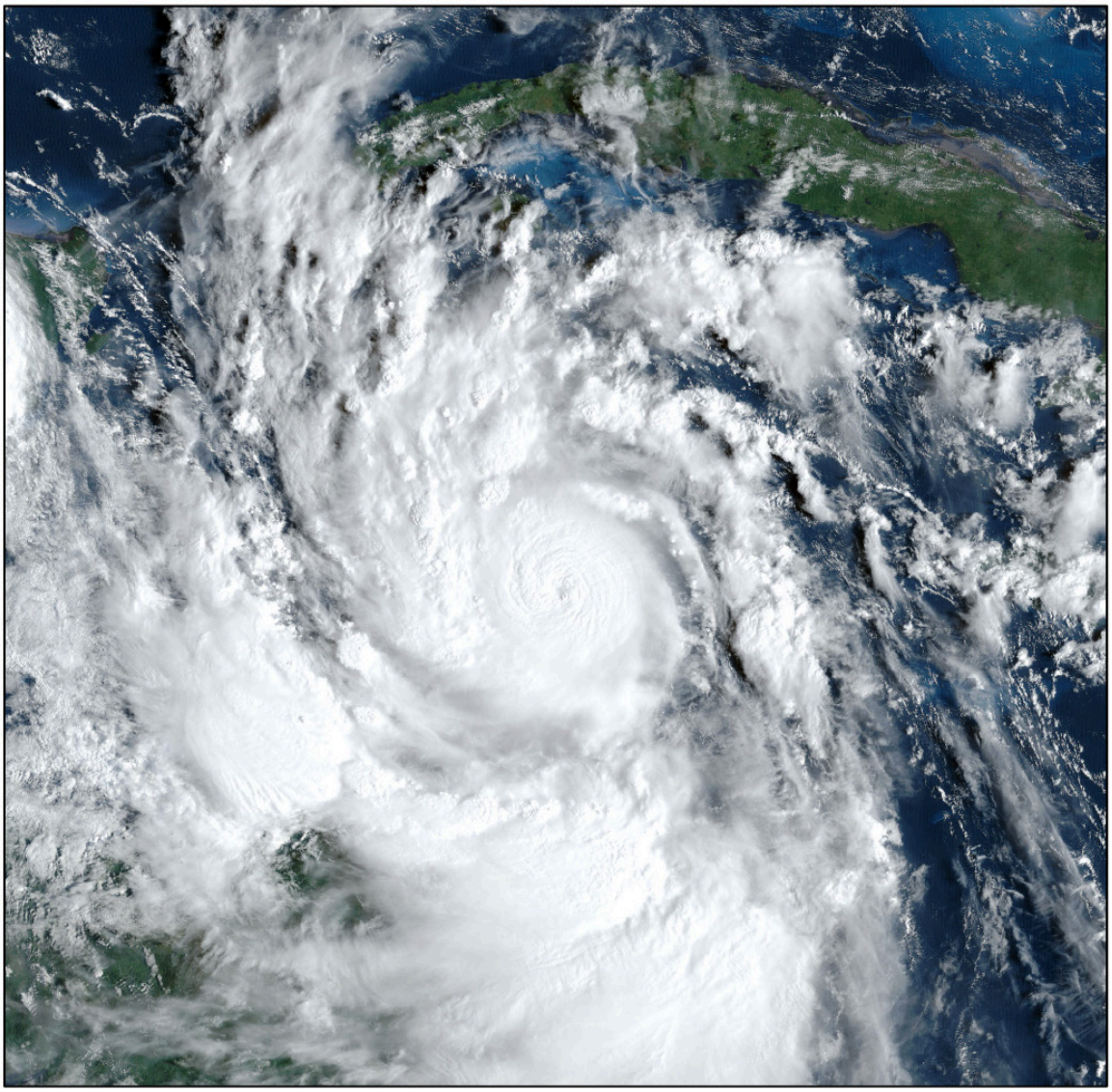

The pinhole eye of Hurricane Delta is nearing its peak intensity of 120 kts at 1330 UTC 6 October.

Figure 21. GOES-16 Geocolor visible satellite image of Hurricane Delta at 1330 UTC 6 October. Source: Cangialosi and Berg (2021).

This RI resulted in a change to the structure of Hurricane Delta. The change in structure can be seen looking at Figure 22, in which there is a sharp decrease in the radius of maximum winds on 5 October (red line in Figure 22), coinciding with an increase in the maximum sustained winds (Figure 23). At the time of Delta's first peak intensity, the radius of maximum winds was approximately 10 nautical miles. Working from the radius of maximum winds (red line) outwards in Figure 22, there is the radius of hurricane force winds of 64 kts (R64; black line), the radius of 50 knot winds (R50; dark blue line), the radius of tropical storm force winds of 34 kts (R34; light blue line), and the radius of the outermost closed isobar (ROCI; green line). The ROCI is determined by measuring the distance from the center of the system to the outermost closed isobar in quadrants. The R34 and ROCI are often used by forecasters to characterize the size of a tropical cyclone's outer circulation. The growth of the tropical cyclone and the increase of the wind radii are important for all water vessels out in the open water. Water vessels should be outside of the 34 kt wind radius to avoid the capsizing of small boats, five-foot or greater seas, and difficulty in controlling or loss of control of water vessels.

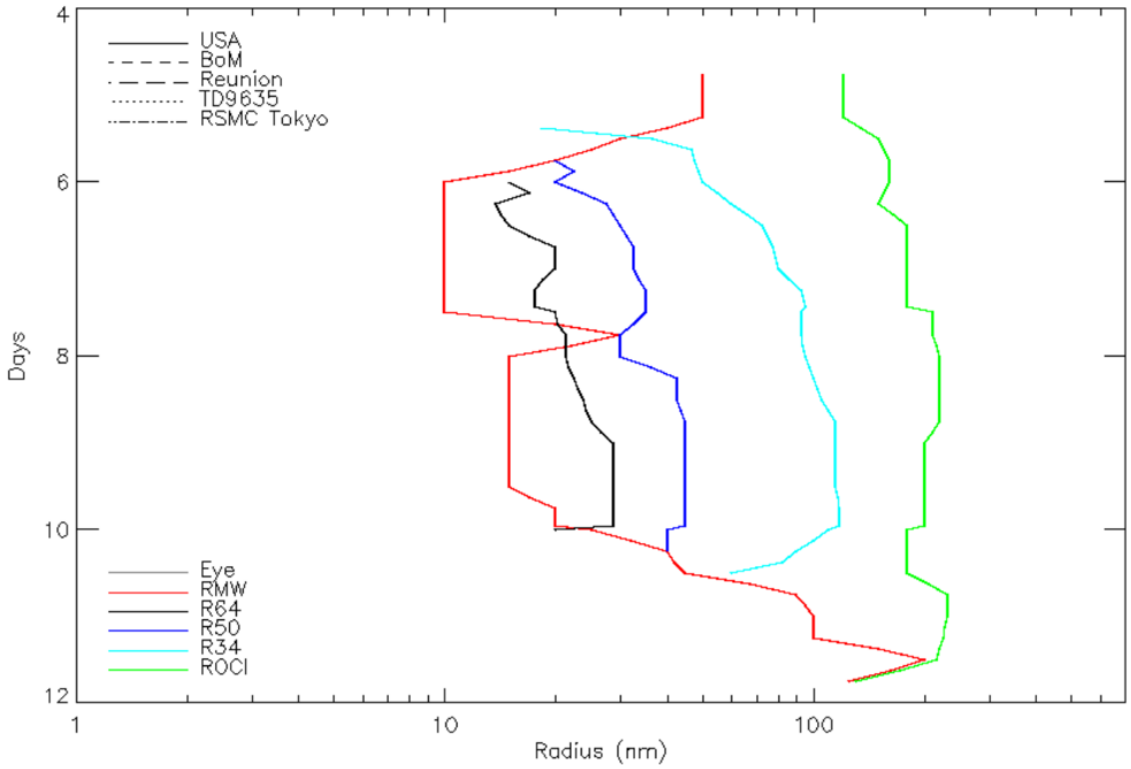

This figure shows the radii from NOAA for the maximum winds (RMW), 64 kts winds (R64), 50 kts winds (R50), 34 kts winds (R34), and the radius of outermost closed isobars (ROCI) as a function of date of October (vertical axis). The radius of the eye is listed but not shown.

Figure 22. Time series of radial wind data. Source:

The wind radii in Figure 23 are indicators of the growth of a tropical cyclone after reaching tropical storm force winds. According to Smith and Montgomery (2023, pg. 399): "As long as the convectively-induced overturning circulation is maintained, the low-tropospheric inflow will continue to flux cyclonic absolute vorticity, both mean and eddy components, inwards, thereby increasing the circulation at a given radius and the mean tangential wind at that radius."

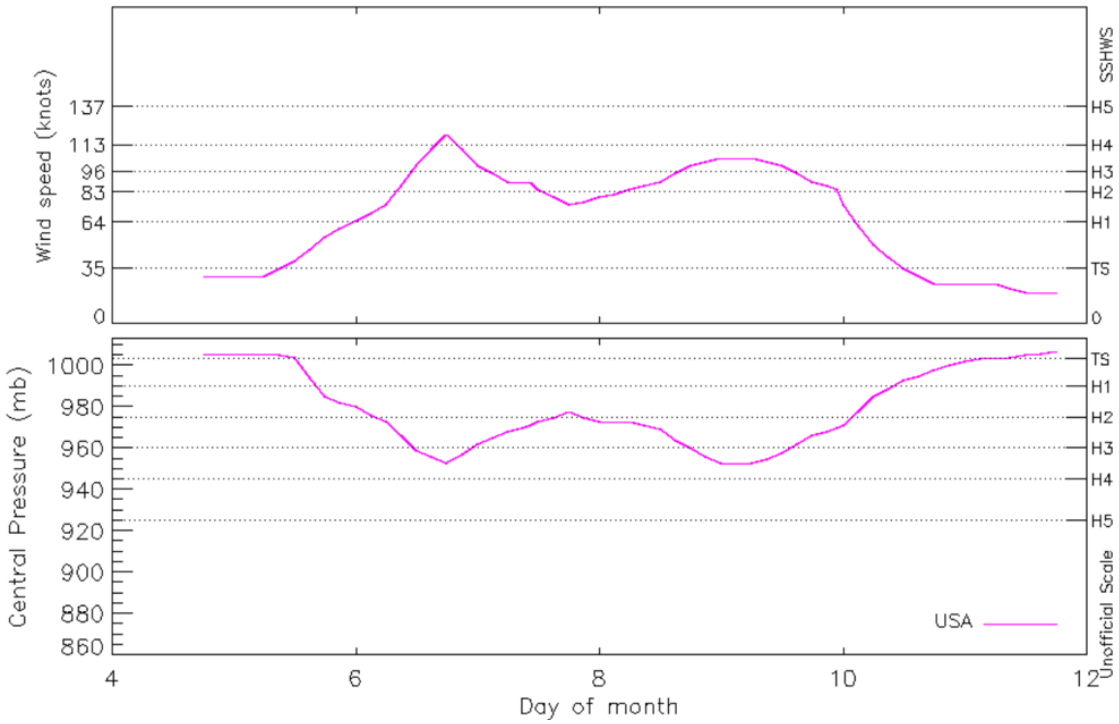

Figure showing the central pressure and wind speed in knots of Hurricane Delta from 5 October 2020, when it was declared a tropical storm to 12 October 2020 when the system returned to tropical storm strength. From this we can see that there were two peaks in Delta's intensity with the first peak occurring more rapidly in intensity. The first peak is then followed by a rather quick weakening phase after peak intensity was reached. The second peak gradually intensified and weakened until the second landfall on late 9 October 2020/early 10 October 2020. The correlation between the increase of intensity with decrease of the systems central pressure is shown.

Figure 23. Time series of storm intensity. Source: Knapp et al. 2010.

It is evident from Figure 23 that the first peak in intensity was followed by a rapid weakening late on 7 October. According to NHC forescaters, this rapid weakening is thought to be due to a sudden increase in vertical wind shear at the mid-levels and dry air intrusion that is evident in the dropsonde data from NOAA and Air Force Hurricane Hunters. However, the frictional interaction of the outer circulation of Hurricane Delta with the northern portion of Cuba and the Yucatan Peninsula may also be a contributer to the weakening of the system.

To gain a better representation of the RH during the rapid weakening, Figure 24 shows the GFS horizontal RH structure at 500 hPa, 700 hPa, 850 hPa, and 925 hPa levels at 00, 06, and 12 UTC 7 October 2020. Throughout the times shown in Figure 24 it can be

seen that the RH is reduced as we move from 925 hPa to 500 hPa. Taking a close look at the 700 hPa and 500 hPa levels, drier air from the west can be seen working its way into the inner circulation of Hurricane Delta. This entrainment of dry air and the increase in the vertical wind shear may have contributed to the weakening of Delta from a category 4 to a category 2 hurricane as it approached the Yucatan Peninsula.

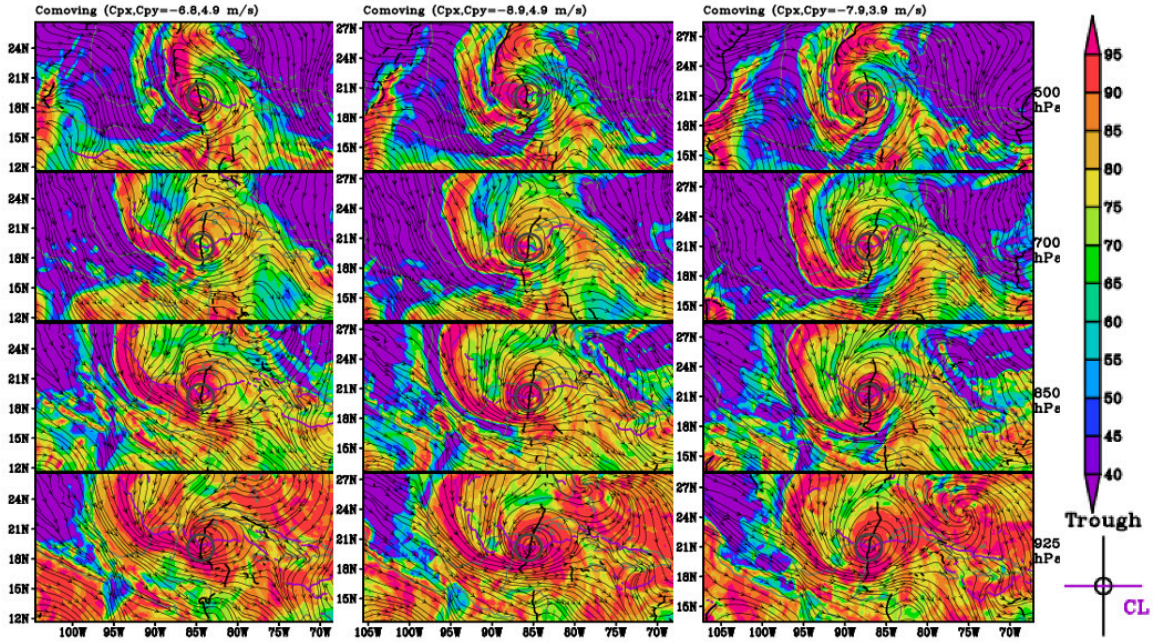

GFS analyses in the co-moving frame of RH from 00 (left), 06 (center), and 12 UTC (right) 7 October 2020 at 500 hPa, 700 hPa, 850 hPa, and 925 hPa with the color bar representing the percentage of RH.

Figure 24. GFS analyses of relative humidity during rapid weakening phase

Figure 25 takes a closer look at the RH at 500 hPa and 700 hPa levels at 00 UTC and 12 UTC 7 October 2020. Drier air can be seen on the west side of the system at the 500 hPa level at 00 UTC 7 October 2020. Over the next 12 hours, the dry air that was on the west side of the system at 500 hPa is surrounding nearly half of the system and is closer to the center of Delta's circulation. At the 700 hPa level, there is a similar pattern, but with RH being slightly higher overall.

The basis for the association between a decreased RH around a storm's core and vortex weakening lies in the hypothesized dynamic-thermodynamic interactions between

a tropical cyclone and its environment. An increase in environmental vertical shear, and related entrainment of dry air above the boundary layer surrounding the cyclone's core, is thought to contribute to vortex weakening via convective downdrafts, which flush the near-core boundary layer with low equivalent potential temperature (θ_e) air originating from above the boundary layer thereby quenching the energy source of the storm in the inflow layer. Since surface fluxes will not fully recover the boundary layer θ_e values relative to a control configuration without dry air entrainment, inflowing air parcels will rise at the base of the eyewall with smaller θ_e values, unable to support a strong vortex.

A conceptual model for the foregoing weakening pathway was proposed and tested in the affirmative by Riemer et al. (2010). Unfortunately, quantitative tests of this weakening mechanism are not possible in a forecast/analysis system that does not explicitly represent deep convection and downdrafts. The conclusion is that whereas the necessary condition for this weakening pathway is satisfied, detailed tests of this pathway require a cloud representing model, which is beyond the scope of this thesis.

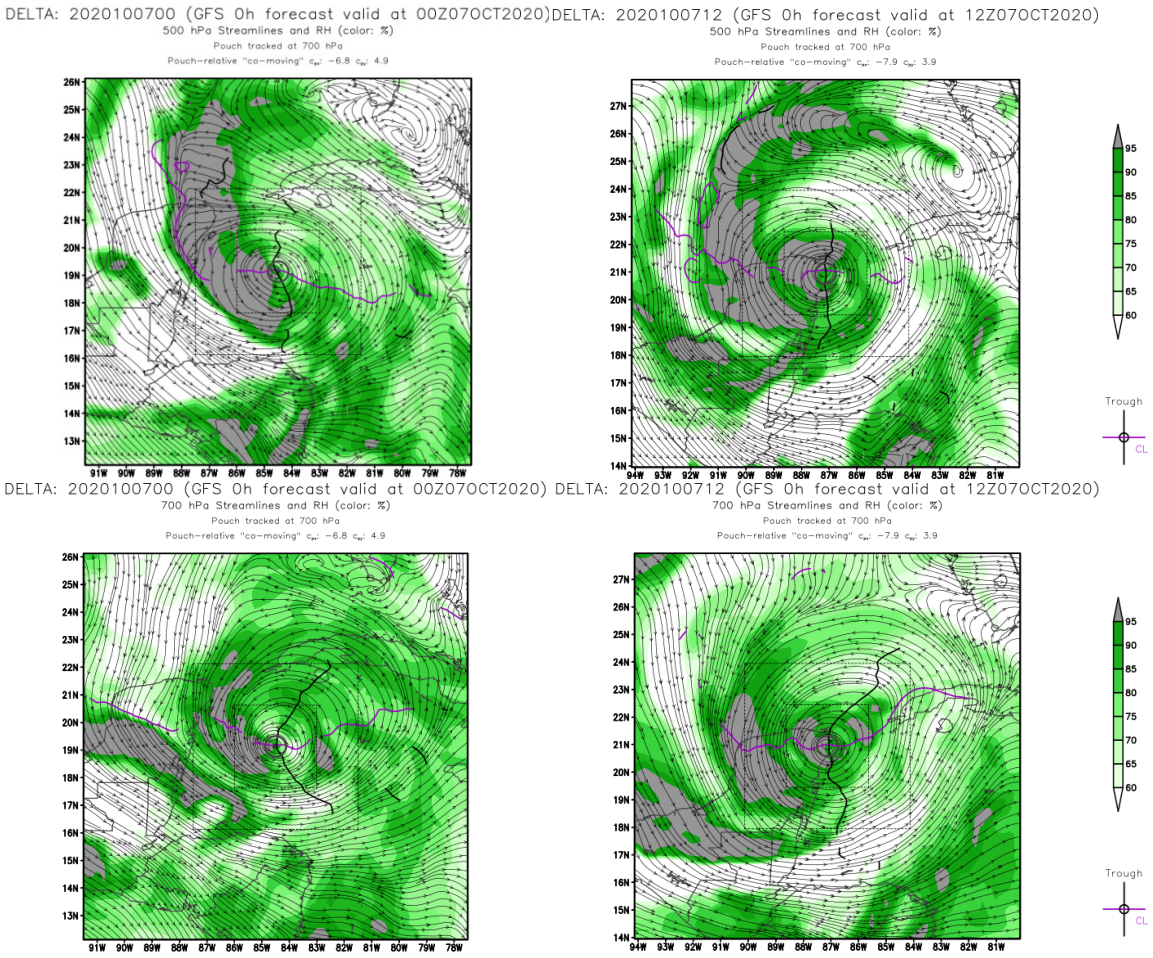

GFS analysis of relative humidity at 500 hPa (top row) and 700 hPa (bottom row) at 00 UTC 7 October 2020 and after initial landfall 60 nautical miles east of Cozumel, Mexico at 12 UTC 7 October 2020. The values of RH are indicated on the right of each row by the color bar.

Figure 25. GFS analysis of relative humidity at 500 hPa and 700 hPa

The second RI occurred shortly after crossing the Yucatan Peninsula and re-entering the Gulf of Mexico. As seen in Figure 23 from Knapp et al. 2010, Delta's wind speeds increased from 75 kts to 105 kts in 30 hours from 1800 UTC 7 October to 0000 UTC 9 October. At the end of this second intensification period, the eye had expanded significantly in size and was observed to be 28 nautical miles in diameter with a symmetrical convective pattern (Figure 26) (Tropical Atlantic). The second increase in intensity was due to Delta moving into a generally more favorable atmospheric environment and oceanic conditions in the Gulf of Mexico after crossing the Yucatan

(Cangialosi and Berg 2021). Looking at Figures 22 and 23, the intensification was a bit more gradual compared to the first RI.

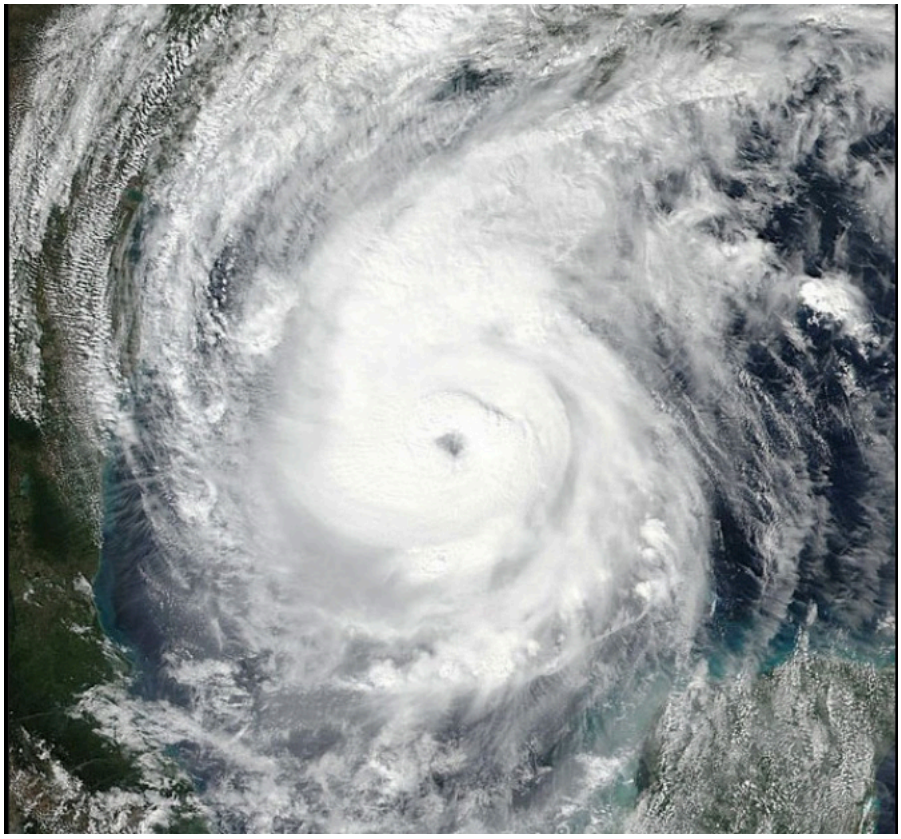

The eye of Hurricane Delta during its second rapid intensification at 1920 UTC 8 October 2020.

Figure 26. NASA TERRA MODIS visible satellite image of Hurricane Delta at 1920 UTC 8 October 2020. Source: Cangialosi and Berg (2021).

D. LANDFALL

Hurricane Delta struck the northeastern portion of the Yucatan Peninsula near Puerto Morelos, Mexico (Figure 27) around 1030 UTC on 7 October 2020 as a Category 2 hurricane with sustained winds of 90 kts and a minimum surface pressure of 971 hPa. Delta maintained its Category 2 intensity during landfall and entered the Gulf of Mexico with 75 kt maximum sustained winds. After entering the Gulf of Mexico, which had generally favorable atmospheric conditions, Delta intensified again and became a Category 3

hurricane. This second intensification occurred in the Gulf of Mexico near 25.3°N 93.5°W. As Delta approached the Louisiana coastline, an increase in vertical wind shear and cooler SSTs of 24.75-26.55°C (NASA Worldview) contributed to the weakening of Delta into a Category 2 hurricane shortly before its second landfall.

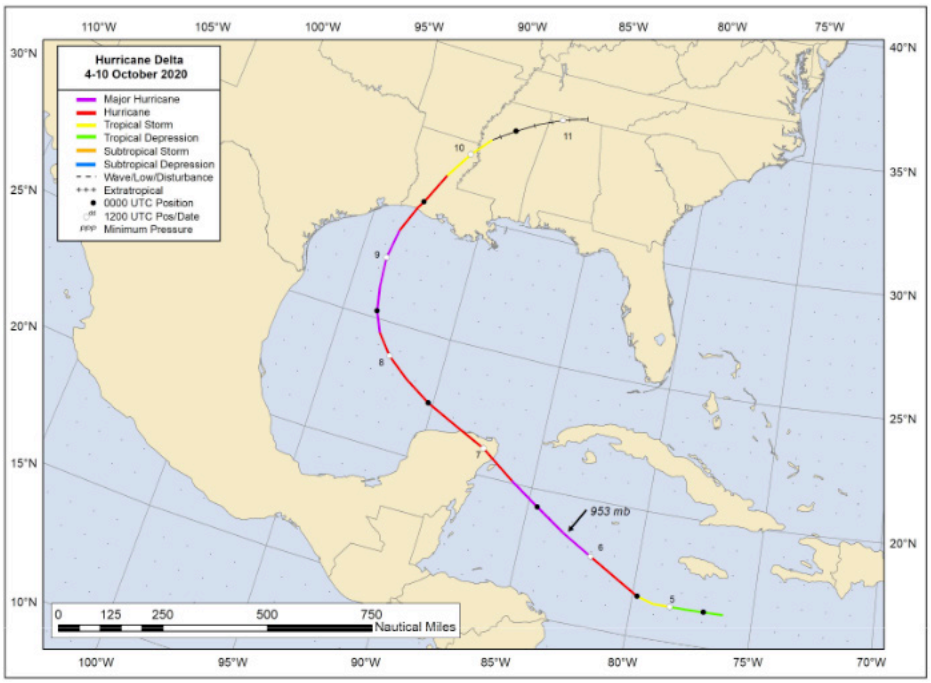

Figure 27. NOAA best track positions for Hurricane Delta, 4–10 October 2020. Source: Cangialosi and Berg (2021).

The second landfall occurred near Creole, Louisiana, at 2300 UTC 9 October 2020 when Delta was a Category 2 hurricane with maximum sustained winds of 85 kts. As Delta was already undergoing weakening from the increased vertical wind shear, the increased friction coefficient from landfall of Delta's eye-eyewall region continued weakening the hurricane. Seven hours after the second landfall, the intensity of Delta was reduced to a tropical storm and Delta continued its northwestward path until 18 UTC 10 October 2020, where it became an extratropical cyclone. The extratropical cyclone continued to lose intensity until it became a low-pressure trough at 00 UTC 12 October 2020.

E. TIME HEIGHT AND TIME-SERIES PLOTS

To support the findings of this investigation, time-height plots of area-averaged relative vorticity, RH, mass flux, and equivalent potential temperature (θ_e) were constructed. Accompanying these time-height plots are time-series plots of area-averaged Okubo-Weiss, relative vorticity, relative humidity, equivalent potential temperature, and upward motion at the tracked 700-hPa level, as well as two calculations of vertical wind shear.

Hurricane Delta's precursor was tracked at 700 hPa from 06 UTC 25 September to 12 UTC 7 October 2020, where relative vorticity was constantly positive in the 6°x6° moving box average. Figure 28 shows the 6°x6° box average for relative vorticity. When the precursor disturbance comes off the African coast, it has an average value of $2.04 \times 10^{-5} s^{-1}$ and was relatively easily tracked for the first two days. As the precursor continued its westward motion across the Atlantic from 28 September 2020 to 2 October 2020, the relative vorticity was still positive, but weaker than its value when coming off the coast of Africa. The weaker averaged cyclonic relative vorticity adds uncertainty in the tracking of the precursor disturbance due to its weak signal. As the precursor crossed into the Lesser Antilles, the signal for relative vorticity became stronger as it entered the more favorable conditions for cyclogenesis in the Caribbean. The increase in the average vorticity increased the certainty of the tracked precursor positions. From 4 October 2020 onwards, the signal for relative vorticity becomes increasingly strong and deepens in the vertical.

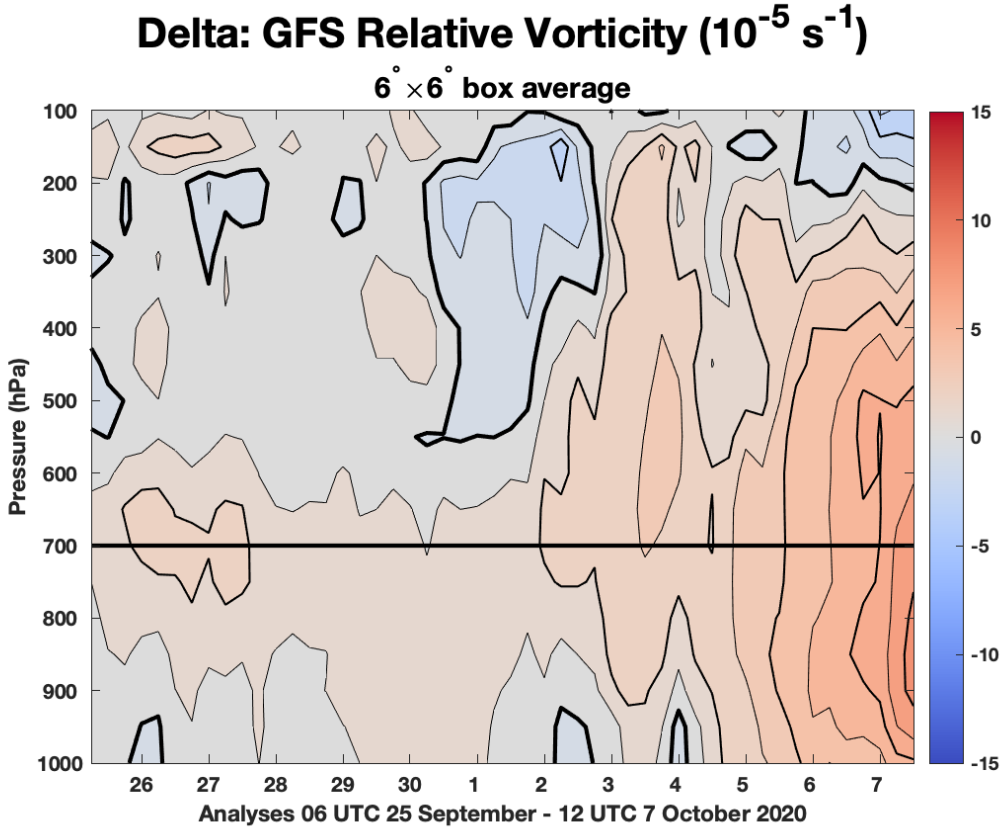

GFS analysis of relative vorticity in the area surrounding Delta's precursor over time in a 6°x6° view. The x axis is representative of the time period the precursor was tracked from 06 UTC 25 September to 12 UTC 7 October 2020. The y axis is representative of pressure levels in hPa with the black horizontal line indicating the tracked level of 700 hPa. The intensity of relative vorticity is indicated by the color bar.

Figure 28. GFS analysis of relative vorticity as a time vs. height plot for Delta's precursor.

The GFS relative humidity averaged over the 6°x6° moving box (Figure 29) shows that, as the precursor was crossing the Atlantic, the average RH was mostly at or around 70%. It wasn't until late on 2 October 2020 that the average RH progressively increased, staying mostly above 80% in the middle and lower levels of the atmosphere. Nearing 6 October 2020, the average RH was 80% or greater, but near the end of 6 October 2020, vertical wind shear began to increase. The increased shear and the associated disturbance-relative flow can open up pathways for dry air to enter the pouch in the mid- and upper-level troposphere. Dry air intrusion can be inferred from Figure 29 between 350 hPa and

500 hPa at the end of the time period. The RH between 350 hPa and 500 hPa shows a decrease from 80% to 60–70%.

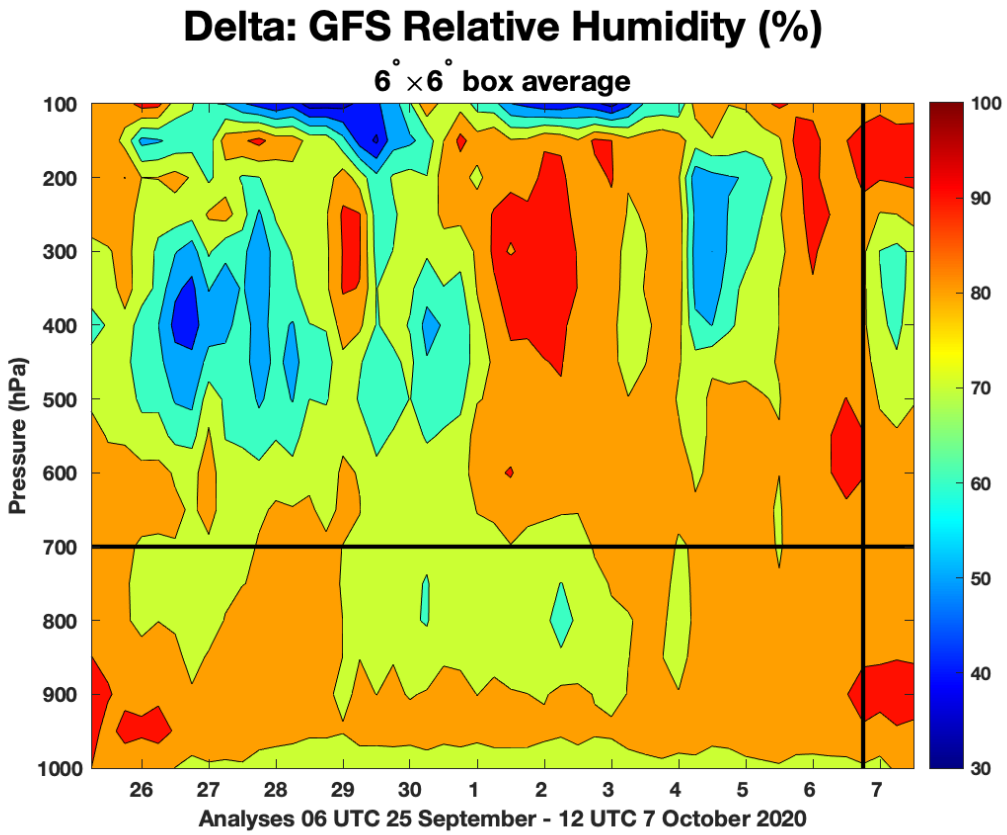

GFS analysis of relative humidity in the area surrounding Delta's precursor over time in a 6°x6° box view. The x axis is representative of the time period the precursor was tracked from 06 UTC 25 September to 12 UTC 7 October 2020.The y axis is representative of pressure levels in hPa with the black horizontal line indicating the tracked level of 700 hPa. The black vertical line indicated the beginning of increased vertical wind shear. The percentage of relative humidity is indicated by the color bar.

Figure 29. GFS analysis of relative humidity as a time vs. height plot for Delta's precursor.

Figure 30 shows that as Delta's precursor disturbance came off the African coast, the upward mass flux from 28 September 2020 to 1 October 2020 was relatively weak. This weakened mass flux coincides with the time period of weak relative vorticity and the period of additional uncertainty in the determined pouch location. From 1 October 2020 to 4 October, a near diurnal mass flux cycle can be seen in Figure 30. After 4 October, the

upward mass flux increases noticeably in the vertical while still exhibiting a near diurnal component. The increase in mass flux is consistent with the moistened air from the boundary layer rising in the troposphere, creating clouds, and releasing latent heat.

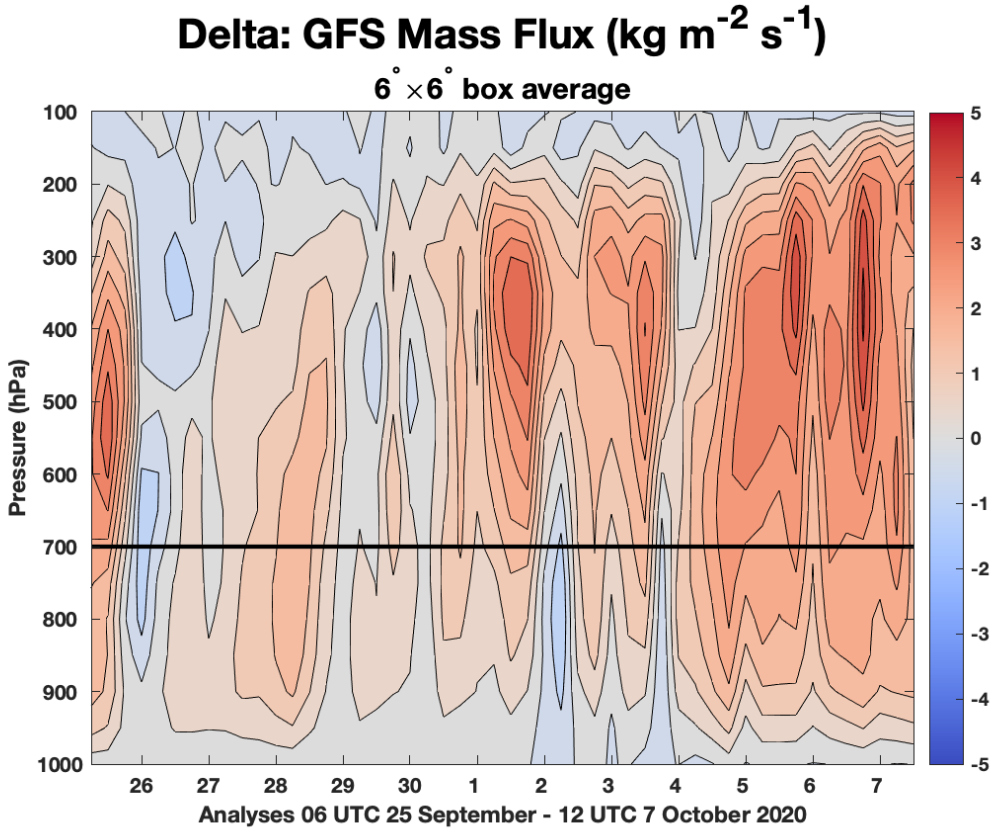

GFS analysis of vertical mass flux in the area surrounding Delta's precursor over time in a 6°x6° box view. The x axis is representative of the time period the precursor was tracked from 06 UTC 25 September to 12 UTC 7 October 2020. The y axis is representative of pressure levels in hPa with the black horizontal line indicating the tracked level of 700 hPa. The strength of the mass flux is indicated by the color bar.

Figure 30. GFS analysis of vertical mass flux as a time vs. height plot for Delta's precursor.

Figure 31 shows the equivalent potential temperature θ_e in an area-averaged, time-height plot. Equation 4 shows the expression used for an unsaturated parcel in which θ_e is conserved in dry adiabatic and pseudoadiabatic displacements.

$$\theta_e \approx \theta \exp\left(L_c q / c_p T_{LCL}\right) \quad (4)$$

where θ is the potential temperature, L_c is the latent heat of condensation, q is the actual mixing ratio of the initial state, c_p is the specific heat at constant pressure, and T_{LCL} is the temperature that the parcel would have if it expanded adiabatically to saturation (Holton 2004).

The θ_e in Figure 31 starts with the typical Atlantic Ocean regime, where θ_e is warmer at the lower and upper levels, but cooler between ~850 to 550 hPa. As the disturbance crossed the Atlantic Ocean, the boundary layer θ_e slowly increases as air parcels acquire additional moisture. After Hurricane Delta was declared at 00 UTC 6 October 2020, the area-averaged θ_e increases throughout the troposphere as moistened air parcels from the boundary layer ascend in deep convective updrafts.

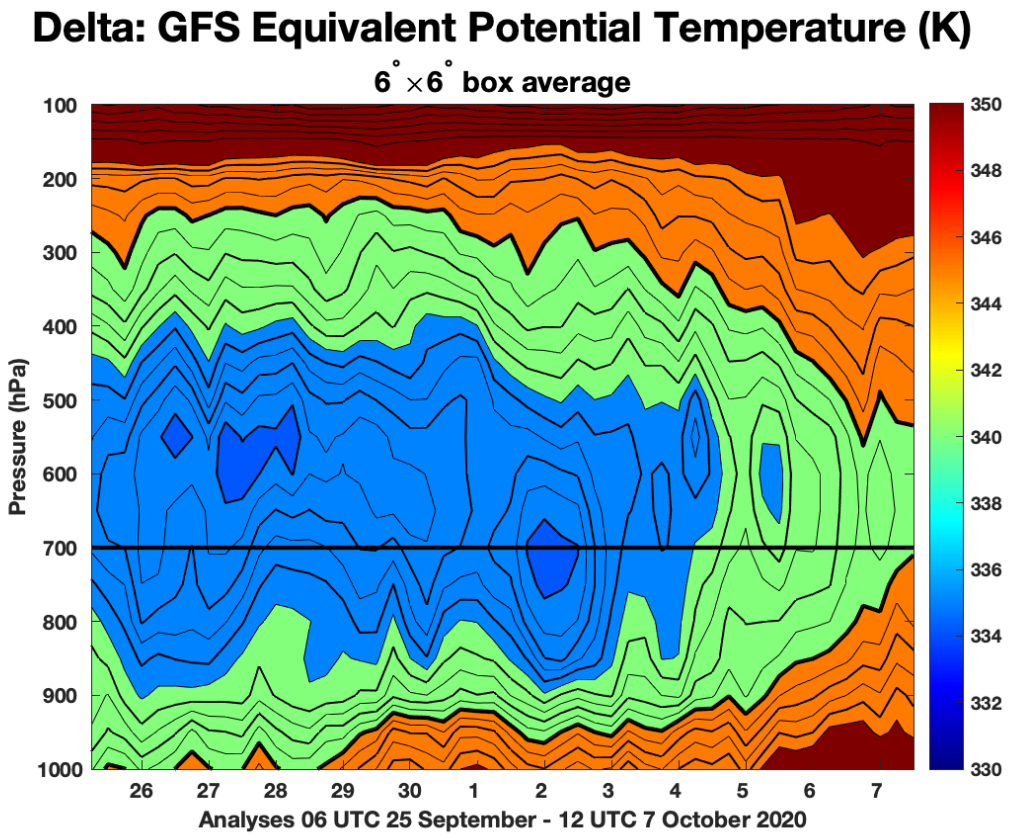

GFS analysis of equivalent potential temperature in the area surrounding Delta's precursor over time in a 6°x6° box view. The x axis is representative of the time period the precursor was tracked from 06 UTC 25 September to 12 UTC 7 October 2020. The y axis is representative of pressure levels in hPa with the black horizontal line indicating the tracked level of 700 hPa. The equivalent potential temperature in Kelvin is indicated by the color bar.

Figure 31. Time-height analysis of equivalent potential temperature (θ_e) for Delta's precursor disturbance using GFS analysis data.

To provide a more complete understanding of the evolution of Delta's precursor, a graphical representation of consolidated data at the tracked 700-hPa level was created as a time series in Figure 32. The top left panel of Figure 32 shows that the precursor disturbance increases its OW and relative vorticity as it approaches the Lesser Antilles on 1 October 2020. The OW has its peak near 18 UTC 6 October, while the relative vorticity peak occurs near 06 UTC 7 October 2020. This peak in OW is the result of the first RI that occurred from approximately 12 UTC 5 October to 18 UTC 6 October 2020. After this

peak in OW there is a rather quick decline, which is representative of the rapid weakening of Delta immediately before landfall.

Shown in the upper right panel is a time series of area-averaged RH and θ_e. An increase of this average θ_e indicates that the air parcels have increased their moisture content, which is beneficial for hurricane formation. The averaged θ_e gradually increases as the disturbance crosses the Lesser Antilles on 2 October 2020, and greatly increases just before Delta's precursor was declared a TD on 4 October 2020. The upward trend in θ_e continues for the remainder of the time period shown.

From the mass flux graph, the diurnal cycle can be seen as mass flux would increase in the nighttime hours and decrease during the daytime hours. On 6 October 2020, a large decrease in mass flux occurred in the 3°x3° box averages. This downward trend in mass flux with time is not present at the tracked 700mb pressure level, but the trend is seen from ~500 mb to 150 mb. As 6 October 2020 went further into the day, the mass flux increased significantly, and the increase coincides with the intensification of Delta to a Category 4 storm with 120 kt sustained winds. A rapid decrease in mass flux is seen subsequently as the storm began to make landfall on the Yucatan Peninsula at approximately 1030 UTC 7 October 2020.

According to hurricane forecasters, in order for a tropical cyclone to form, intensify and maintain itself, vertical wind shear should be no more than approximately 10 m s^{-1} (~20 knots) between 5,000 and 38,00 feet (850 hPa – 200 hPa), respectively. Although this condition serves as a useful "rule of thumb," this approximate threshold holds an important caveat: It does not guarantee that the environment will be unfavorable if shear is over 10 m s^{-1} because the size of a tropical cyclone plays a role also in determining if there will be a negative effect on the cyclone's development. Specifically, a large tropical cyclone may not feel the negative impacts from the shear even if it is higher than the 10 m s^{-1} threshold. The resiliency of a storm to vertical wind shear can be strengthened by the presence of high relative humidity in the middle troposphere surrounded by the storm's pouch. This moist envelope protects the circulation from dry air entrainment and the high θ_e helps maintain the warm core system.

The pouch 500–850 hPa vertical shear (Figure 32, lower right, red dashed and solid lines) values suggest that as the wave-pouch disturbance approached the Caribbean (from 30 September on) there are several occurrences where the pouch shear increases and decreases, but the pouch shear does not increase beyond 10 m s^{-1} until early on 5 October 2020. The lowest pouch shear in this period occurs on and around 4 October and this correlates well with the formation of the TD on this same day. On 5 October 2020, a TS is declared and correlates to a time when the shear was more favorable. As the pouch shear decreased at 12 UTC 5 October 2020, an RI phase began. During this RI phase, Hurricane Delta was declared at 00 UTC 6 October 2020 and continued until 18 UTC 6 October, at which time Delta became a category 4 hurricane. After this RI phase, the pouch shear increased ~10 m s^{-1}, which is believed to have led to the rapid weakening of the storm by approximately 30 kts.

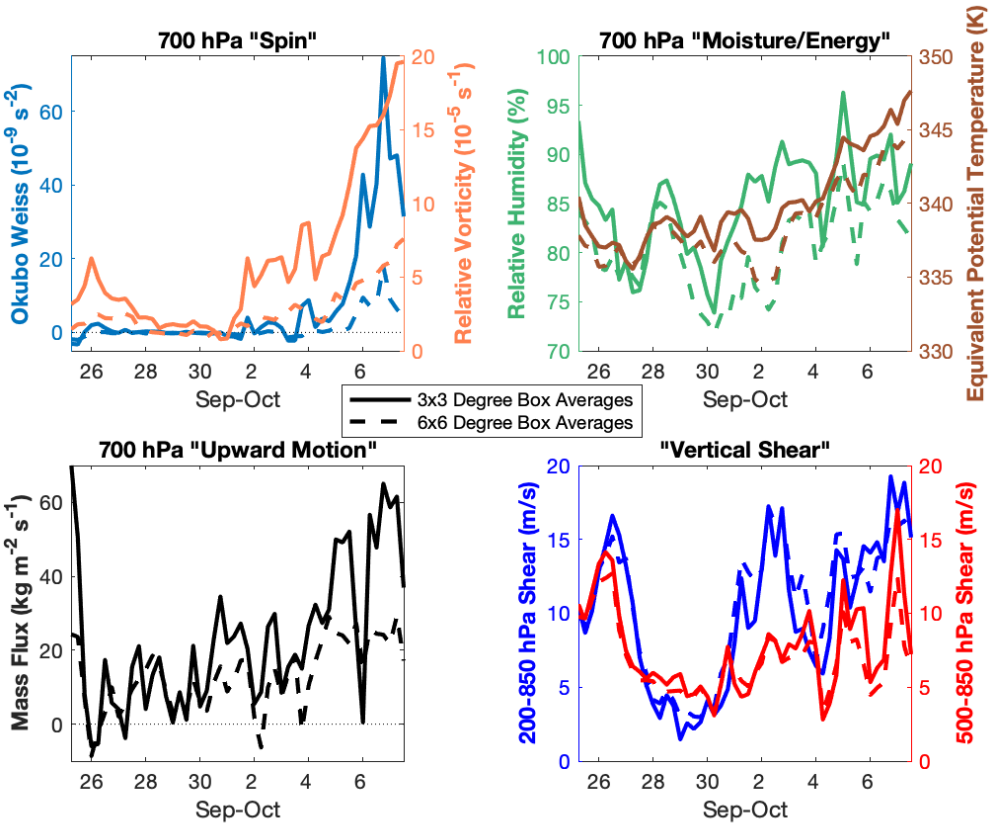

Pouch-centered box-averaged GFS analysis values of Okubo-Weiss and relative vorticity (upper left), relative humidity and equivalent potential temperature (upper right), mass flux (bottom left), and vertical shear for the deep and pouch atmosphere (bottom right) for the precursor of and eventual Hurricane Delta. Time tracked includes 06 UTC 25 September to 12 UTC 7 October 2020. Solid line depicts the 3x3 degree box while the dashed line depicts the 6x6 degree box.

Figure 32. GFS time series plots of Delta's precursor for Okubo-Weiss, relative vorticity, relative humidity, equivalent potential temperature, mass flux and vertical shear

IV. CONCLUSIONS

All tropical cyclones are unique in their formation, but have the commonality of being a powerful, deadly force that can end lives, destroy property, and deteriorate the ability of our military to protect our country. Tropical cyclones pose a challenge to all forecasters and the Marsupial Paradigm aims to provide forecasters with a better understanding of the processes that govern tropical cyclone formation and new tools to analyze candidate disturbances. The Marsupial Paradigm offers a model on pouches and how these pouches can protect the nascent tropical cyclone from adverse effects of the environmental vertical wind shear and dry air entrainment; such protected sub-regions allow for the development of persistent deep convection. This deep convection is what enables a disturbance to be nurtured and become a self-sustaining tropical cyclone. Tracking Hurricane Delta from time of hurricane formation back to the coast of Africa was a long, drawn-out, time-consuming task, that required several revisitations of multiple time periods to ensure proper positions and phase speeds. Highlights of the precursor's evolution from the African coast to the formation of a tropical cyclone in the Caribbean are as follows.

Pouches are associated with deep convection, though pouch positions are not always aligned with the deep convection. This is especially true during the early nurturing phase of a pouch. Though this is not new information, it is helpful in identifying potential areas of pouch locations via the persistent convective activity. Convection near a forming shallow pouch or wave-trough may not be clearly associated with a specific pouch location but may be associated with the wave-trough going through a relatively high moisture content area.

For cyclogenesis to occur, pouches must exist at middle and lower levels and be relatively aligned in the vertical for further development. As seen with Delta, which was tracked at 700 hPa, the existence of the pouch at a single level is not adequate for tropical cyclone development. This observation strengthens the Marsupial Paradigm's first hypothesis of "bottom-up" development of cyclogenesis. To be clear, the structure of a pouch does not need to begin at the low levels, but a pouch's structure must ultimately

extend into the lower levels for convergence of cyclonic vorticity to occur near the surface. Delta's precursor pouch was well moistened throughout the column and required the extension of the pouch to lower levels for further development and cyclogenesis. The synoptic scale interactions with Hurricane Gamma, paired with the amplification of the Bermuda High, acted to reduce the phase speed of Delta's precursor and changed its path southwestward for some time. This stalling phase is thought to have allowed the pouch's influence to extend into the lower levels, which enabled a vertically aligned system.

After the vertical alignment of the pouches and the strengthening into a tropical storm, Delta underwent a RI of 90 kts in under 36-hours as it continued into favorable (warm) SSTs and relatively low vertical wind shear. Shortly after Hurricane Delta became a category 4 hurricane with maximum sustained winds of 120 kts, the system encountered an increase in mid-level vertical wind shear. As the wind shear persisted, intrusion of dry air occurred. The infiltration of dry air is suggested to have contributed to the rapid weakening of Delta from a category 4 to a category 2 hurricane, 60 nautical miles east of Cozumel, Mexico. Shortly after, Delta made its first landfall near Puerto Morelos, Mexico, as a category 2 hurricane.

A. OPERATIONAL IMPACTS

Operationally, the Marsupial Paradigm can help forecasters add context to their narrative of a tropical cyclone formation. In the co-moving reference frame, insight into a disturbances' structure can be provided prior to the Earth-relative reference frame, satellite detection, and imagery. Shifting from the Earth-relative to the co-moving framework allows forecasters the ability to improve their accuracy of the position of a candidate developing disturbance. Specifically, the application of phase speed(s) to a parent wave allows for the identification of the preferred area of cyclonic development ahead of the formation of a TD by hours or even days.

With the ability to detect and identify cyclonic development earlier than the current methods at forecasting centers, warnings can be sent out earlier and preparations can be initiated sooner. Early preparation can save lives and reduce the impact to civilian and military property alike. Being able to move valuable military assets ahead of a hurricane is

important in reducing damage to said assets and ensuring that our military readiness is not affected by the devastation that hurricanes can cause.

B. OPPORTUNITIES FOR FUTURE WORK

This study is unique as it tracked the path of Hurricane Delta's precursor using the Marsupial Paradigm from the Caribbean Sea back to its origin on the African coast. The precursor pouch was tracked for 10 days prior to it being declared a TD. Using the Marsupial Paradigm to track tropical cyclones back to their origin off the African coast and investigating what wave features are present before TD formation offers potentially useful information about what wave characteristics favor tropical cyclogenesis.

The automated pouch tracker run by the Montgomery Research Group at the Naval Postgraduate School in Monterey, California provides forecasts out to 120 hours. These forecasts cover the North Atlantic, eastern North Pacific, western North Pacific, North Indian, South Indian, and South Pacific basins. The tracker for these six major TC basins is run once a day using the 00 UTC operational GFS. The Montgomery Research Group provides plots of the forecast GFS variables using similar pressure-level charts that have been included in this thesis of co-moving streamlines with OW, relative vorticity and RH, as well as the time-height plots of these variables. In addition, the group produces a probability for each pouch developing into a TC in 3-hour intervals out to 120 hours. The automated pouch tracker's performance of the probability forecast tool has yet to be assessed.

THIS PAGE INTENTIONALLY LEFT BLANK

LIST OF REFERENCES

Asaadi, A., G. Brunet, and M. K. Yau, 2016a: On the Dynamics of the Formation of the Kelvin Cat's-Eye in Tropical Cyclogenesis. Part I: Climatological Investigation. *J. Atmospheric Sci.*, **73**, 2317–2338, https://doi.org/10.1175/JAS-D-15-0156.1.

Asaadi, A., G. Brunet, and M. K. Yau, 2016b: On the Dynamics of the Formation of the Kelvin Cat's-Eye in Tropical Cyclogenesis. Part II: Numerical Simulation. *J. Atmospheric Sci.*, **73**, 2339–2359, https://doi.org/10.1175/JAS-D-15-0237.1.

Asaadi, A., G. Brunet, and M. K. Yau, 2017: The Importance of Critical Layer in Differentiating Developing from Nondeveloping Easterly Waves. *J. Atmospheric Sci.*, **74**, 409–417, https://doi.org/10.1175/JAS-D-16-0085.1.

Bister, M., and K. A. Emanuel, 2002: Low frequency variability of tropical cyclone potential intensity 1. Interannual to interdecadal variability. *J. Geophys. Res. Atmospheres*, **107**, https://doi.org/10.1029/2001JD000776.

Cangialosi, J., and R. Berg, 2021: Hurricane Delta (AL262020).

Dunkerton, T. J., M. T. Montgomery, and Z. Wang, 2009: Tropical cyclogenesis in a tropical wave critical layer: easterly waves. *Atmos Chem Phys*, **9**, 5587–5646.

Gilford, D. M., 2021: pyPI (v1.3): Tropical Cyclone Potential Intensity Calculations in Python. *Geosci. Model Dev.*, **14**, 2351–2369, https://doi.org/10.5194/gmd-14-2351-2021.

Holton, J. R., 2004: *An Introduction to Dynamic Meteorology*. 4th ed. Elsevier Academic Press, 535 pp.

Kim, H.-S., D.-S. R. Park, C.-H. Ho, I.-J. Moon, and J. C. L. Chan, 2022: Latitudinal Variation of the Lifetime Maximum Intensity Location of Atlantic Tropical Cyclones Controlled by the Atlantic Multidecadal Oscillation. *Geophys. Res. Lett.*, **49**, e2021GL097459, https://doi.org/10.1029/2021GL097459.

Klotzbach, P. J., and Coauthors, 2022: A Hyperactive End to the Atlantic Hurricane Season October–November 2020. *Bull. Am. Meteorol. Soc.*, **103**, E110–E128, https://doi.org/10.1175/BAMS-D-20-0312.1.

Knapp, K. R., M. C. Kruk, D. H. Levinson, H. J. Diamond, and C. J. Neumann, 2010: The International Best Track Archive for Climate Stewardship (IBTrACS): Unifying Tropical Cyclone Data. *Bull. Amer. Meteor. Soc.*, **91**, 363–376, https://doi.org/10.1175/2009BAMS2755.1.

Li, X., Z.-Z. Hu, Y. Tseng, Y. Liu, and P. Liang, 2022: A Historical Perspective of the La Niña Event in 2020/2021. *J. Geophys. Res. Atmospheres*, **127**, e2021JD035546, https://doi.org/10.1029/2021JD035546.

McWilliams, J. C., and G. R. Flierl, 1979: On the Evolution of Isolated, Nonlinear Vortices. *J. Phys. Oceanogr.*, **9**, 1155–1182, https://doi.org/10.1175/1520-0485(1979)009<1155:OTEOIN>2.0.CO;2.

NASA Worldview, SOTO by Worldview. https://soto.podaac.earthdatacloud.nasa.gov/?v=-98.87880859375,24.91767578125,-90.52041015625,30.74482421875&l=Reference_Labels_15m(hidden),Reference_Features_15m(hidden),Coastlines_15m,MODIS_Aqua_L2_Chlorophyll_A(hidden),GHRSST_L4_MUR_Sea_Surface_Temperature_Anomalies(hidden),GHRSST_L4_MUR_Sea_Surface_Temperature(min=24.6,squash=true),MODIS_Aqua_CorrectedReflectance_TrueColor(hidden)&lg=true&s=-93.8,27.5%2B-93.6,28.7%2B-93.1,29.8&t=2020-10-08-T16%3A45%3A36Z (Accessed December 11, 2022).

National Weather Service, 2021: Background Information: The North Atlantic Hurricane Season. *Natl. Weather Sevice Clim. Predict. Cent.*,. https://www.cpc.ncep.noaa.gov/products/outlooks/hurricane2003/August/background_information.html (Accessed September 29, 2022).

NHC, Atlantic Basin Hurricane Tracking Chart. https://www.nhc.noaa.gov/images/tracking_chart_atlantic.png (Accessed October 15, 2022).

NOAA, 2020: La Nina develops during peak hurricane season. *Natl. Ocean. Atmospheric Adm.*,. http://www.noaa.gov/news/la-nina-develops-during-peak-hurricane-season (Accessed August 31, 2022).

NOAA AOML, 2005: Frequently Asked Questions About the Atlantic Multidecadal Oscilation (AMO). https://www.aoml.noaa.gov/phod/amo_faq.php (Accessed October 1, 2022).

Rice, D., 2008: Storm alert: “Pouches” protect embryonic hurricanes. August 18.

Riemer, M., M. T. Montgomery, and M. E. Nicholls, 2010: A new paradigm for intensity modification of tropical cyclones: thermodynamic impact of vertical wind shear on the inflow layer. *Atmospheric Chem. Phys.*, **10**, 3163–3188, https://doi.org/10.5194/acp-10-3163-2010.

Rouault, E., and Coauthors, 2022: GDAL. https://doi.org/10.5281/ZENODO.6801315.

Samost, A., 2006: Predicting Hurricanes. https://web.mit.edu/12.000/www/m2010/teams/neworleans1/predicting%20hurricanes.htm (Accessed August 26, 2022).

Schmit, T. J., P. Griffith, M. M. Gunshor, J. M. Daniels, S. J. Goodman, and W. J. Lebair, 2017: A Closer Look at the ABI on the GOES-R Series. *Bull. Am. Meteorol. Soc.*, **98**, 681–698, https://doi.org/10.1175/BAMS-D-15-00230.1.

Tropical Atlantic, Delta (2020) Recon – Atlantic – Tropical Atlantic. http://tropicalatlantic.com/recon/recon.cgi?basin=al&year=2020&storm=Delta (Accessed October 26, 2022).

University of Wisconsin – CIMSS, CIMSS Tropical Cyclones Group. https://tropic.ssec.wisc.edu.

Ventrice, M. J., C. D. Thorncroft, and P. E. Roundy, 2011: The Madden–Julian Oscillation's Influence on African Easterly Waves and Downstream Tropical Cyclogenesis. *Mon. Weather Rev.*, **139**, 2704–2722, https://doi.org/10.1175/MWR-D-10-05028.1.

THIS PAGE INTENTIONALLY LEFT BLANK

INITIAL DISTRIBUTION LIST

1. Defense Technical Information Center
   Ft. Belvoir, Virginia

2. Dudley Knox Library
   Naval Postgraduate School
   Monterey, California